Supporting Information for

A Class of Electron-Deficient Units: Fluorenone Imide and Its Electron-Withdrawing Group-Functionalized Derivatives

Zhicai Chen,[⊥] Yu Zhang,[⊥] Pu Wang,[⊥] Jiaxin Yang, Kun Yang, Jianfeng Li, Jie Yang, Yongchun Li, Huanli Dong* and Xugang Guo*

Dr. Z. Chen, Dr. K. Yang, Dr. J. Li, J. Yang, Y. Li, Prof. X. Guo

Department of Materials Science and Engineering, Southern University of Science and Technology (SUSTech), No. 1088, Xueyuan Road, Shenzhen, Guangdong 518055, China

E-mail: guoxg@sustech.edu.cn (X.G.)

Y. Zhang, P. Wang, J. Yang, Prof. H. Dong

Beijing National Laboratory for Molecular Science, Key Laboratory of Organic Solids, Institute of Chemistry, Chinese Academy of Sciences, Beijing 100190, China

E-mail: dhl522@iccas.ac.cn (H.D.)

Content

1. Measurements and instruments

Nuclear magnetic resonance (NMR) spectra were recorded on a Bruker Ultra Shield Plus AV400 spectrometer (^{1}H NMR 400 MHz and ^{13}C NMR 100 MHz) or Bruker Avance 500 MHz or on a Bruker Avance 600 MHz spectrometer with $CDCl_3$ or DMSO-d_6 or THF-d_8 as the solvents and tetramethylsilane (TMS) as the internal standard. High resolution mass spectrometry (HRMS) measurements were performed on a Thermo Scientific Q-Exactive mass spectrometer. Melting point (m. p.) of the compounds were recorded on an SGW X-4A micro melting point apparatus. UV-vis absorption spectra were recorded on a Shimadzu UV-3600 UV-VIS-NIR spectrophotometer.

2. Materials

All reagents and chemicals were purchased from Energy Chemical., Admas-beta, and Bide pharmatch Ltd., *etc*, and used as received without further purification unless otherwise specified. Anhydrous THF and toluene were distilled from Na/benzophenone under argon. Unless otherwise stated, all reactions were carried out under inert atmosphere using standard Schlenk line techniques.

3. Synthetic procedure

The synthetic procedures of the intermediates and target products were illustrated in **Scheme S1** and **S2**. Compound **2**-**4** were prepared according to the previous literature with high yields [1, 2]. The preparation of compound **6** from compound **4** was performed according to the previous literature [3].

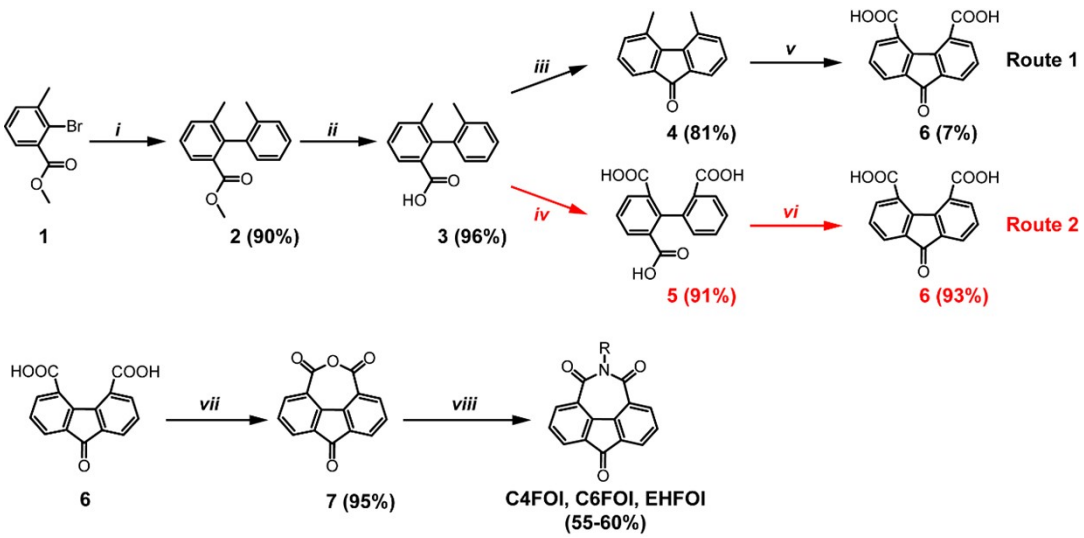

Scheme S1. Synthetic route to fluorenone imide and its derivatives, reagents and conditions: *i*) methyl 2-bromo-3-methylbenzoate acid, $Pd_2(dba)_3$, S-phos, K_2CO_3, toluene/EtOH/H_2O, 90 °C; *ii*) NaOH (aq), reflux; *iii*) $MeSO_3H$, 110 °C; *iv*) $KMnO_4$ (aq), CTMAB, 100 °C, then HCl; *v*) $KMnO_4$, H_2O/pyridine, 100 °C; *vi*) PPA, 130 °C; *vii*) Ac_2O, 130 °C; *viii*) alkyl primary amine, DMAP, 1, 4-dioxane, 90 °C, then Ac_2O, 130 °C.

[1, 1'-Biphenyl]-2, 2', 6-tricarboxylic acid (compound **5):**

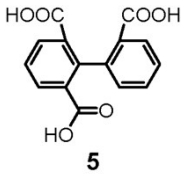

5

2',6-Dimethyl-[1,1'-biphenyl]-2-carboxylic acid **3** (20 mmol, 4.52 g), cetyltrimethylammonium bromide (CTMAB) (0.10 mmol, 0.36 g) and water (500 mL) were added to a 1 L two-necked round bottom. The reaction mixture was heated to 90 °C and $KMnO_4$ (120 mmol, 9.46 g) was added slowly in several portions. The mixture was stirred overnight and stopped until the dark red color of $KMnO_4$ faded. The resulting mixture was filtered to give a colorless aqueous phase and then concentrated to ~150 mL under a reduced pressure. 10 mL concentrated HCl was carefully added to the resulting solution and a white solid precipitated. After filtration, the solid was collected and dried overnight in a vacuum drying oven to give compound **5** as a white powder (5.21 g, 91% yield). ^{1}H NMR (400 MHz, DMSO-d_6): δ ppm 12.46 (s, 3H), 7.92

(d, J = 7.8 Hz, 3H), 7.48 (br, 2H), 7.39 (t, J = 7.6 Hz, 1H), 7.00 (d, J = 6.5 Hz, 1H). ^{13}C NMR (100 MHz, DMSO-d_6): δ ppm 167.95, 167.27, 142.40, 141.50, 132.41, 131.61, 130.86, 130.23, 129.82, 129.49, 126.79, 126.71. HRMS (m/z): Calcd. for $C_{15}H_9O_6$ [M-H]$^-$, Exact Mass: 285.0405; Found: 285.0401, m. p. 243-244 °C.

9-Oxo-9H-fluorene-4, 5-dicarboxylic acid (compound **6):**

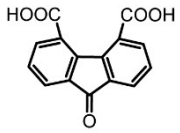

6

Route 2:

Polyphosphoric acid (PPA, 40 mL) and compound **5** (2.86 g，10 mmol) were stirred at 120 ºC for 12 h. After cooled to room temperature, 100 mL ice water was added to the mixture and then stirred for 1 h. After filtration, the resulting solid was washed by water and dried overnight in a vacuum drying oven to give compound **6** as a light-brown powder (2.42 g, 93% yield) ^{1}H NMR (400 MHz, DMSO-d_6): δ ppm 13.18 (s, 2H), 7.90 (d, J = 7.7, 2H), 7.82 (d, J = 7.3, 2H), 7.53 (t, J = 7.5 Hz, 2H). ^{13}C NMR (100 MHz, DMSO-d_6) δ ppm 191.18, 167.85, 142.76, 135.41, 135.19, 131.22, 129.81, 125.93. HRMS (m/z): Calcd. for $C_5H_7O_5$ [M-H]$^-$, Exact Mass: 267.0299; Found: 267.0295, m. p. 285-286 °C.

9-Oxo-9H-fluorene-4, 5-dicarboxylic acid (compound 7):

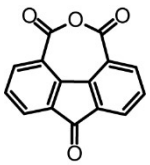

7

Compound **6** (600 mg, 2.24 mmol) was stirred in 20 mL acetic anhydride under reflux for 12 h. After cooled to room temperature, the solid was collected by filtration, washed with methanol, and dried in vacuum overnight to afford a light-brown solid as the compound **7**, which can be used for the following reaction without further purification (530 mg, 95%).

9-Butylfluoreno[4,5-*cde*]azepine-4,8,10(*9H*)-trione (compound C4FOI):

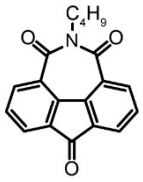

C4FOI

Compound **7** (500 mg, 2.0 mmol), butan-1-amine (175 mg, 2.40 mmol) and DMAP (292 mg, 2.40 mmol) were added into a flask with 20 mL anhydrous 1, 4-dioxane. The resulting mixture was heated to 90 °C for overnight, and the reaction turned into a clear solution and 5 mL acetic anhydride was then added in one portion. The mixture was heated to 130 °C and stirred for another 6 h. After cooled to room temperature, 100 mL water was added and the mixture was extracted with dichloromethane (DCM) three times and the combined organic layer was dried over Na_2SO_4. The solvent was removed under a reduced pressure to afford a residue, which was purified by column chromatography over silica gel using petroleum ether (PE):DCM (3:1) as the eluent to afford the target compound as a withe solid (370 mg, 60%). ^{1}H NMR (400 MHz, $CDCl_3$): δ ppm 8.46 (dd, *J* = 8.1, 0.9 Hz, 2H), 7.94 (dd, *J* = 7.2, 0.9 Hz, 2H), 7.58 (dd, *J* = 7.9, 7.4 Hz, 2H), 4.33-4.25 (m, 2H), 1.82-1.68 (m, 2H), 1.51-1.42 (m, 2H), 1.00 (t, *J* = 7.4 Hz, 3H). ^{13}C NMR (125 MHz, $CDCl_3$) δ ppm 190.73, 164.74, 140.27, 138.34, 133.73, 130.92, 128.67, 127.48, 47.74, 30.07, 20.52, 13.88. HRMS (m/z): Calcd. for $C_{19}H_{16}NO_3$ $[M+H]^+$, Exact Mass: 306.1125; Found: 306.1118, m. p. 98-99 °C.

9-Hexylfluoreno[4,5-*cde*]azepine-4,8,10(*9H*)-trione (compound C6FOI):

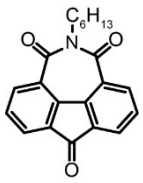

C6FOI

C6FOI was prepared following the same procedure for **C4FOI** (58%). ^{1}H NMR (400 MHz, $CDCl_3$): δ ppm 8.46 (d, *J* = 8.1 Hz, 2H), 7.95 (d, *J* = 7.1 Hz, 2H), 7.63 – 7.54 (m, 2H), 4.32 – 4.23 (m, 2H), 1.83-1.70 (m, 2H), 1.52 – 1.29 (m, 6H), 0.91 (t, *J* = 7.0 Hz,

3H). ^{13}C NMR (125 MHz, $CDCl_3$): δ ppm 190.74, 164.73, 140.27, 138.35, 133.73, 130.92, 128.67, 127.49, 47.99, 31.56, 27.94, 26.94, 22.65, 14.08. HRMS (m/z): Calcd. for $C_{21}H_{20}O_3N$ $[M+H]^+$, Exact Mass: 334.1438; Found: 334.1428, m. p. 103-104 °C.

9-(2-Ethylhexyl)fluoreno[4,5-*cde*]azepine-4,8,10(*9H*)-trione (compound EHFOI):

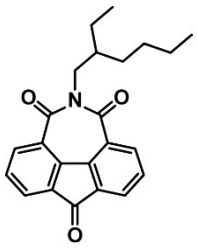

EHFOI

EHFOI was prepared following the same procedure for **C4FOI** (55%). ^{1}H NMR (400 MHz, $CDCl_3$): δ ppm 8.45 (dd, *J* = 8.2, 1.0 Hz, 2H), 7.95 (dd, *J* = 7.2, 1.0 Hz, 2H), 7.58 (dd, *J* = 8.1, 7.3 Hz, 2H), 4.39 (dd, *J* = 8.4, 7.3 Hz, 2H), 1.90 – 1.79 (m, 1H), 1.41 – 1.21 (m, 8H), 0.95-0.83 (m, 6H). ^{13}C NMR (100 MHz, $CDCl_3$): δ ppm 190.74, 165.27, 140.19, 138.41, 133.71, 130.91, 128.63, 127.67, 50.39, 38.01, 30.76, 28.64, 24.07, 23.13, 14.09, 10.73. HRMS (m/z): Calcd. for $C_{23}H_{24}O_3N$ $[M+H]^+$, Exact Mass: 362.1751; Found: 362.1753, m. p. 115-116 °C.

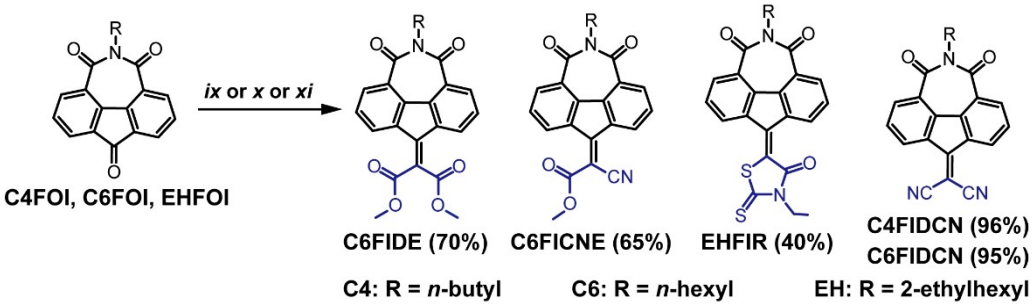

Scheme S2. Synthetic routes to imide-functionalized fluorenone derivatives, *ix*) dimethyl malonate or methyl 2-cyanoacetate, $TiCl_4$, pyridine, $CHCl_3$, rt; *x*) 3-ethyl-2-thioxothiazolidin-4-one, *β*-alanine, HOAc/toluene, 120 °C; *xi*) malononitrile, DMSO, 120 °C.

Dimethyl2-(9-hexyl-8,10-dioxo-9,10-dihydrofluoreno[4,5-*cde*]azepin-4(*8H*)-ylidene)malonate (C6FIDE):

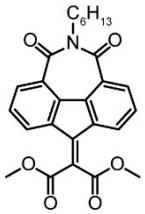

C6FIDE

C6FOI (333 mg, 1 mmol), dimethyl malonate (396 mg, 3 mmol) and 3 mL pyridine in 30 mL DCM was stirred at 0 °C. Then 0.5 mL $TiCl_4$ was added slowly to the mixture and the reaction misture was stirred at room temperature overnight. 100 mL water was added and the mixture was extracted with dichloromethane (DCM) three times, the combined organic layer was dried over Na_2SO_4. The solvent was removed under a reduced pressure to afford a residue, which was purified by column chromatography over silica gel using PE:DCM (3:1) as the eluent to afford the target compound as a light yellow solid (313 mg, 70%). ^{1}H NMR (400 MHz, $CDCl_3$): δ ppm 8.39 (dd, *J* = 8.1, 0.8 Hz, 2H), 8.07 (dd, *J* = 7.8, 0.7 Hz, 2H), 7.49 (t, *J* = 8.0 Hz, 2H), 4.32 – 4.21 (m, 2H), 4.00 (s, 6H), 1.82 – 1.69 (m, 2H), 1.49 – 1.28 (m, 6H), 0.90 (t, *J* = 7.0 Hz, 3H). ^{13}C NMR (100 MHz, THF-d_8) δ ppm 165.50, 165.35, 141.61, 138.15, 136.25, 135.43, 130.50, 129.65, 128.09, 125.67, 53.21, 47.97, 32.37, 28.54, 27.67, 23.35, 14.24. HRMS (m/z): Calcd. for $C_{26}H_{25}O_6N$ $[M]^-$, Exact Mass: 447.1682; Found: 447.1684, m. p. 125-126 °C.

Methyl2-cyano-2-(9-hexyl-8,10-dioxo-9,10-dihydrofluoreno[4,5-*cde*]azepin-4(*8H*)-ylidene)acetate (C6FICNE):

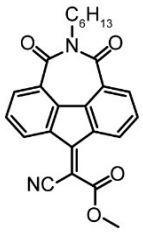

C6FICNE

C6FOI (250 mg, 0.75 mmol), methyl 2-cyanoacetate (223 mg, 2.25 mmol) and 3 mL pyridine in 30 mL DCM was stirred at 0 °C. Then 0.5 mL $TiCl_4$ was added slowly to the mixture and the reaction misture was stirred at room temperature overnight. 100 mL water was added and the mixture was extracted with dichloromethane (DCM) three

times, the combined organic layer was dried over Na_2SO_4. The solvent was removed under a reduced pressure to afford a residue, which was purified by column chromatography over silica gel using PE:DCM (3:1) as the eluent to afford the target compound as a light yellow solid (202 mg, 65%). ^{1}H NMR (400 MHz, $CDCl_3$): δ ppm 8.86 (d, *J* = 7.8 Hz, 1H), 8.48 – 8.33 (m, 3H), 7.59 (t, *J* = 8.0 Hz, 1H), 7.49 (t, *J* = 8.0 Hz, 1H), 4.31 – 4.20 (m, 2H), 4.06 (s, 3H), 1.83 – 1.69 (m, 2H), 1.48 – 1.28 (m, 6H), 0.91 (t, *J* = 7.0 Hz, 3H). ^{13}C NMR (150 MHz, THF-d_8) δ ppm 164.90, 164.85, 162.84, 151.87, 138.45, 138.41, 137.06, 136.99, 136.04, 134.81, 132.62, 130.51, 130.38, 130.19, 128.29, 128.21, 116.28, 102.73, 54.03, 48.13, 32.34, 28.44, 27.67, 23.35, 14.23. HRMS (m/z): Calcd. for $C_{25}H_{22}O_4N_2$ $[M]^-$, Exact Mass: 414.1585; Found: 414.1585, m. p. 126-127 °C.

4-(3-Ethyl-4-oxo-2-thioxothiazolidin-5-ylidene)-9-(2-ethylhexyl)fluoreno[4,5-*cde*]azepine-8,10(*4H,9H*)-dione (EHFIR):

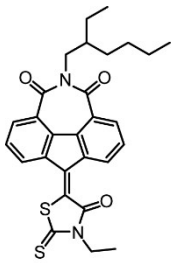

EHFIR

EHFOI (180 mg, 0.5 mmol), rhodanine (160 mg, 1 mmol), and *β*-alanine (76.0 mg, 0.85 mmol) were dissolved in a mixture of glacial acetic acid (10 mL) and toluene (10 mL) and the reaction mixture was stirred at 118 °C for 18 h. Upon cooled to room temperature, the mixture was diluted with water (100 mL) and extracted with $CHCl_3$ (3 ×15 mL). The combined organic layer was washed with $NaHCO_3$ saturated solution until no gas formation was observed, dried over anhydrous Na_2SO_4 and filtered. The solvent was removed under a reduced pressure to afford a residue, which was purified by column chromatography over silica gel using PE:DCM (3:1) as the eluent to afford the target compound as a light yellow solid (100 mg, 40%). ^{1}H NMR (400 MHz, $CDCl_3$): δ ppm 9.59 (d, *J* = 8.0 Hz, 1H), 8.35 (dd, *J* = 8.1, 3.9 Hz, 2H), 8.07 – 8.00 (m, 1H), 7.56 (td, *J* = 8.0, 4.5 Hz, 2H), 4.43 – 4.24 (m, 4H), 1.87 (m,1H), 1.43 – 1.21 (m,

11H), 0.96 – 0.81 (m, 6H). ^{13}C NMR (150 MHz, THF-d_8) δ ppm 191.03, 166.65, 165.87, 165.67, 138.32, 138.24, 137.96, 137.40, 135.98, 135.50, 134.89, 133.74, 131.40, 130.24, 129.72, 128.42, 128.14, 127.86, 50.39, 40.72, 38.80, 31.54, 29.34, 24.76, 23.81, 14.27, 12.15, 10.88. HRMS (m/z): Calcd. for $C_{28}H_{28}O_3N_2S_2$ $[M]^-$, Exact Mass: 504.1547; Found: 504.1549, m. p. 135-136 °C.

2-(9-Butyl-8,10-dioxo-9,10-dihydrofluoreno[4,5-*cde*]azepin-4(*8H*)-ylidene) malononitrile (C4FIDCN):

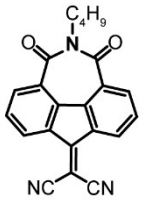

C4FIDCN

Compound **C4FOI** (305 mg, 1.0 mmol) and malononitrile (100 mg, 1.5 mmol) were dissolved in 4 mL DMSO and the mixture was stirred at 120 °C for 24 h. After cooled to room temperature, 20 mL de-ionized water was added to the reaction. Then the resulted mixture was filtered and washed with acetonitrile to give the crude product **C4FIDCN** as light yellow precipitate. The crude product was further purified with column chromatography to afford the target compound as a light yellow solid (335 mg, 96%). ^{1}H NMR (400 MHz, $CDCl_3$): δ ppm 8.69 (d, J = 7.7 Hz, 2H), 8.50 (d, J = 8.2 Hz, 2H), 7.62 (t, J = 8.0 Hz, 2H), 4.3-4.23 (m, 2H), 1.80-1.68 (m, 2H), 1.52-1.40 (m, 2H), 1.00 (t, J = 7.4 Hz, 3H). ^{13}C NMR (100 MHz, THF-d_8) δ ppm 164.61, 158.15, 138.62, 138.38, 134.71, 131.17, 130.80, 128.76, 113.64, 79.52, 47.97, 30.65, 21.13, 14.04. HRMS (m/z): Calcd. for $C_{22}H_{15}N_3O_2$ $[M]^-$, Exact Mass: 353.1170; Found: 353.1171, m. p. 188-189 °C.

2-(9-Hexyl-8,10-dioxo-9,10-dihydrofluoreno[4,5-*cde*]azepin-4(*8H*)-ylidene)malononitrile (C6FIDCN):

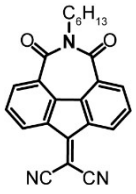

C6FIDCN

C6FIDCN was prepared following the same procedure for **C4FIDCN** (95%). ^{1}H NMR (400 MHz, $CDCl_3$): δ ppm 8.69 (d, *J* = 7.7 Hz, 2H), 8.50 (d, *J* = 8.2 Hz, 2H), 7.62 (t, *J* = 8.0 Hz, 2H), 4.33-4.18 (m, 2H), 1.75 (dt, *J* = 15.4, 7.5 Hz, 2H), 1.49-1.30 (m, 6H), 0.91 (t, *J* = 6.9 Hz, 3H). ^{13}C NMR (100 MHz, THF-d_8) δ ppm 164.71, 158.31, 138.75, 138.36, 134.82, 131.13, 130.82, 128.86, 113.69, 79.53, 48.17, 32.33, 28.45, 27.64, 23.34, 14.22. MALDI-TOF MS: Calcd. for $C_{24}H_{19}N_3O_2$ $[M]^-$, Exact Mass: 381.1483; Found: 381.1480, m. p. 199-200 °C.

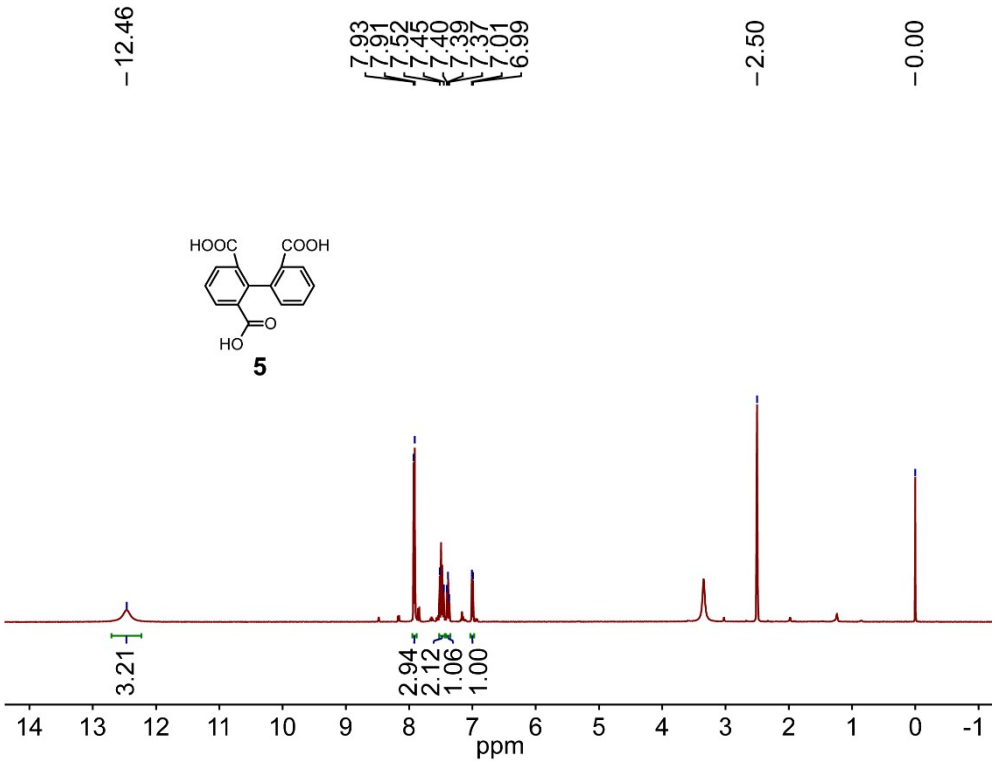

Fig. S1. ^{1}H NMR spectrum of compound **5** in DMSO-d_6.

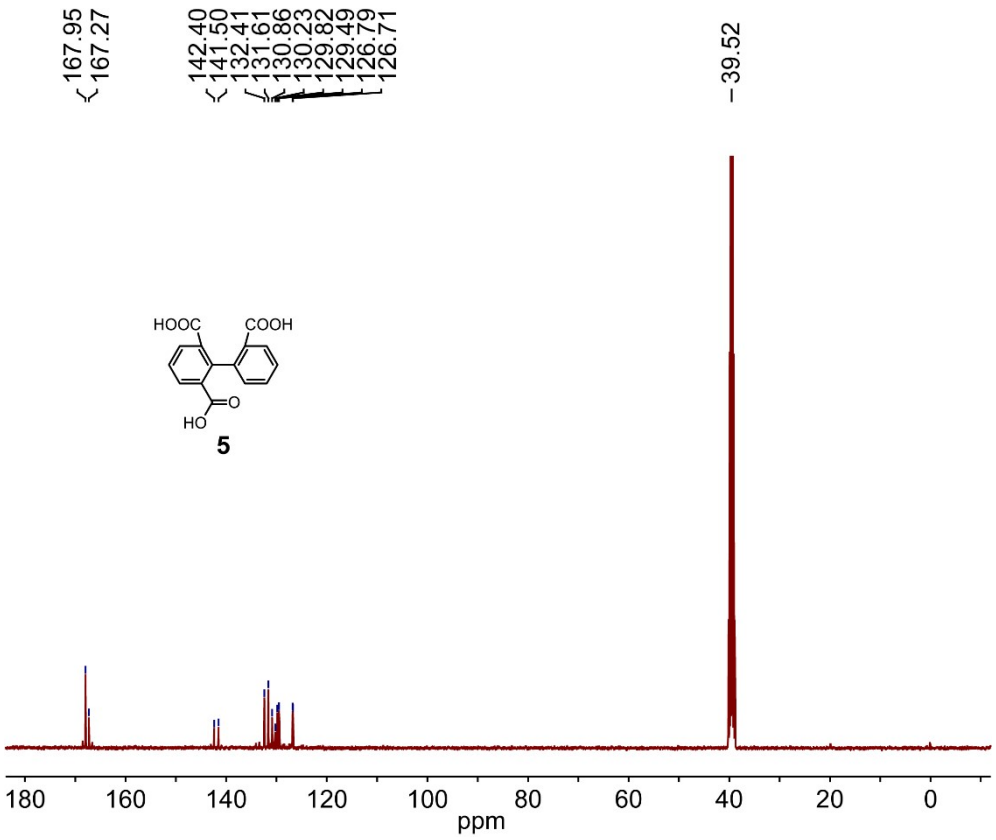

Fig. S2. ^{13}C NMR spectrum of compound **5** in DMSO-d_6.

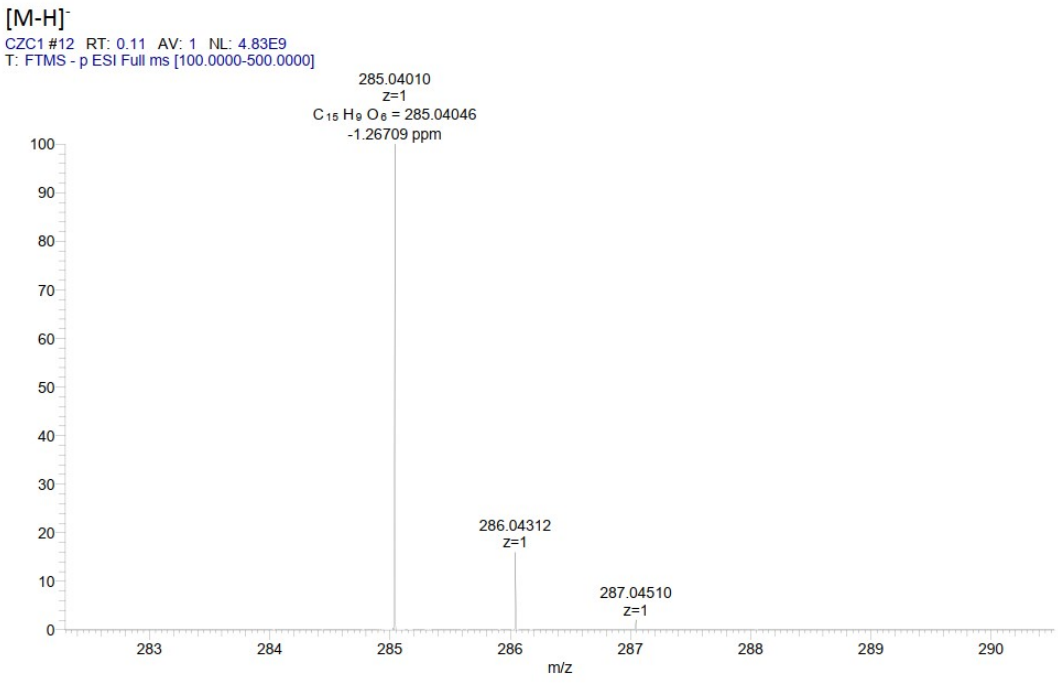

Fig. S3. High-resolution mass spectrum of compound **5** (negative mode).

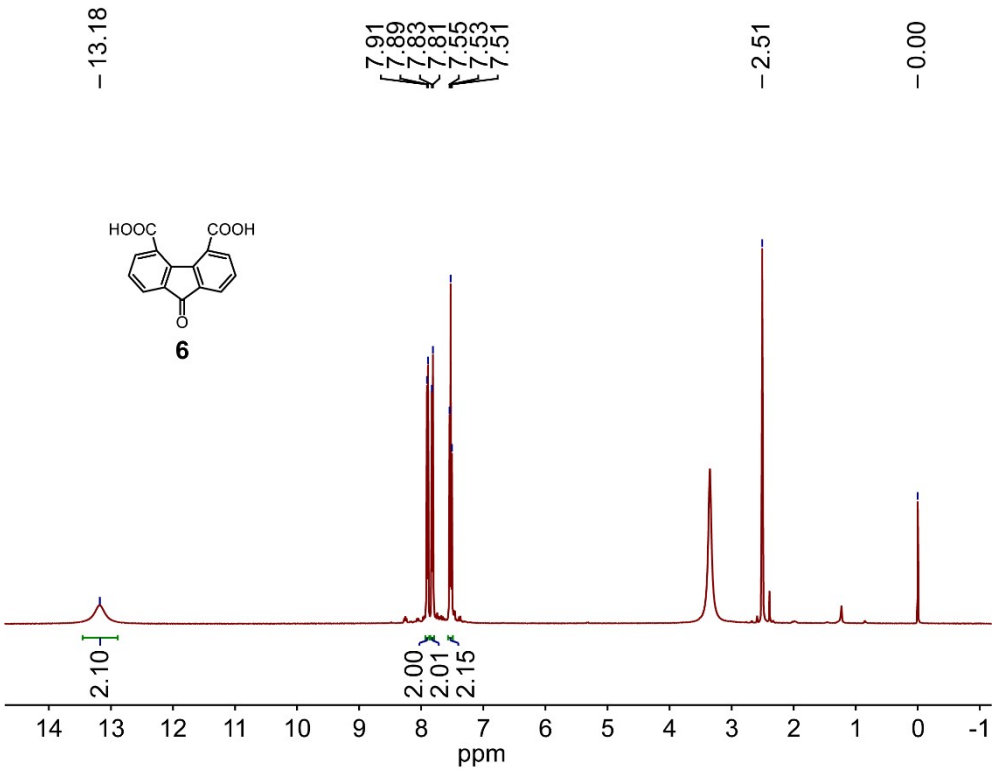

Fig. S4. [1]H NMR spectrum of compound **6** in DMSO-d_6.

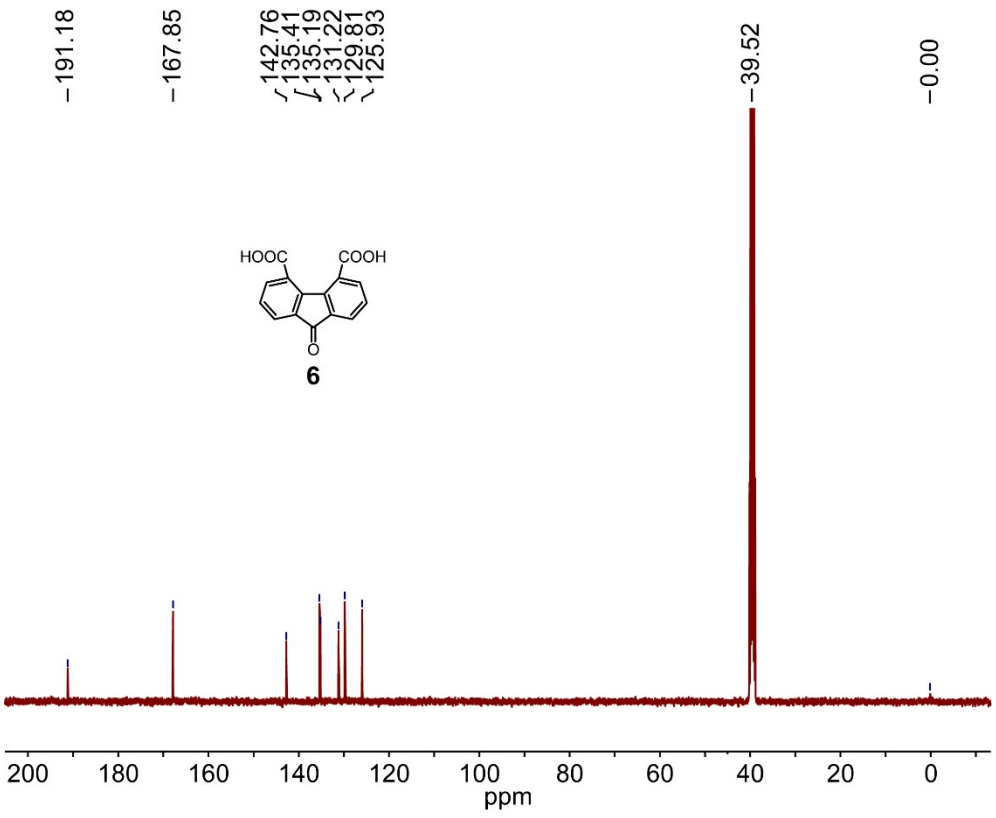

Fig. S5. ^{13}C NMR spectrum of compound **6** in DMSO-d_6.

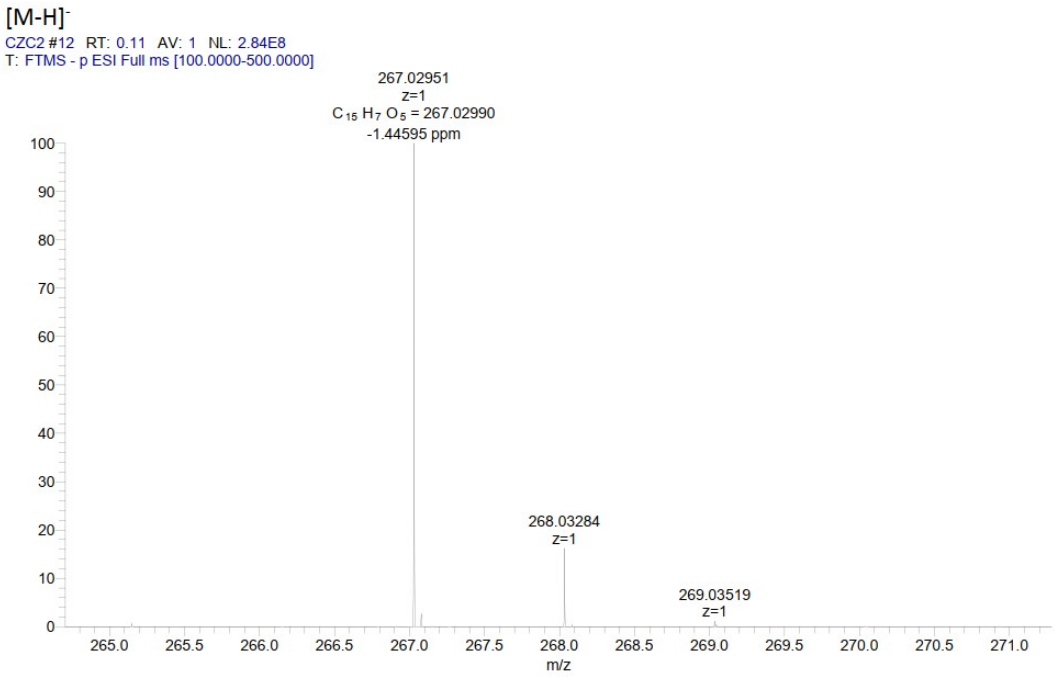

Fig. S6. High-resolution mass spectrum of compound **6** (negative mode).

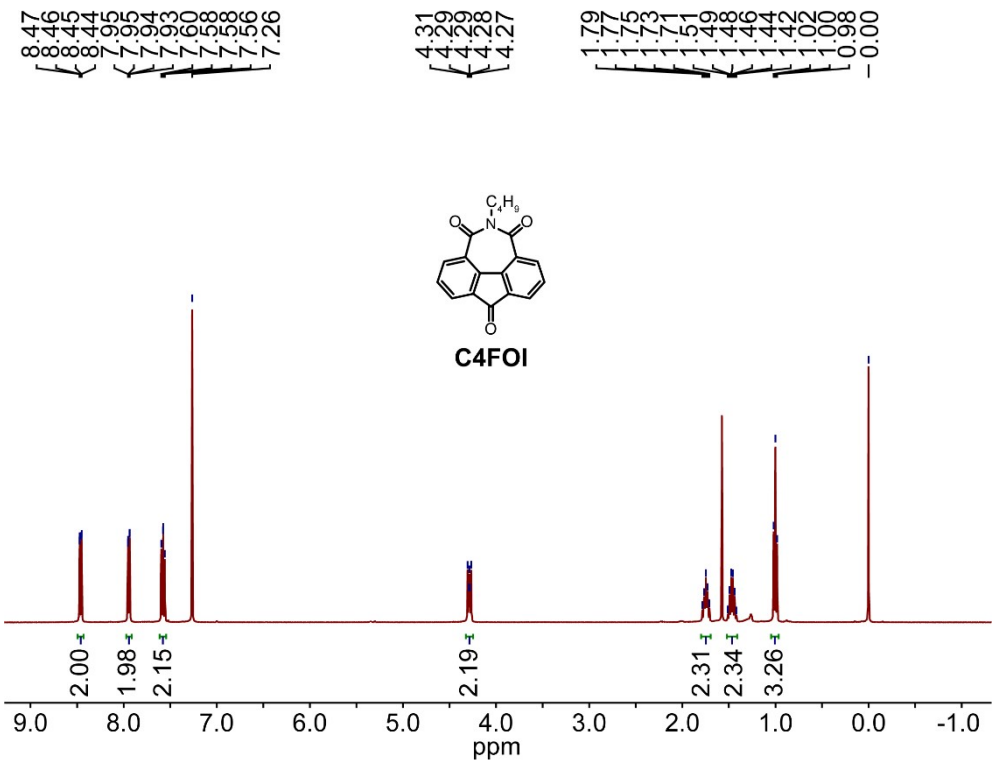

Fig. S7. ^{1}H NMR spectrum of compound **C4FOI** in $CDCl_3$.

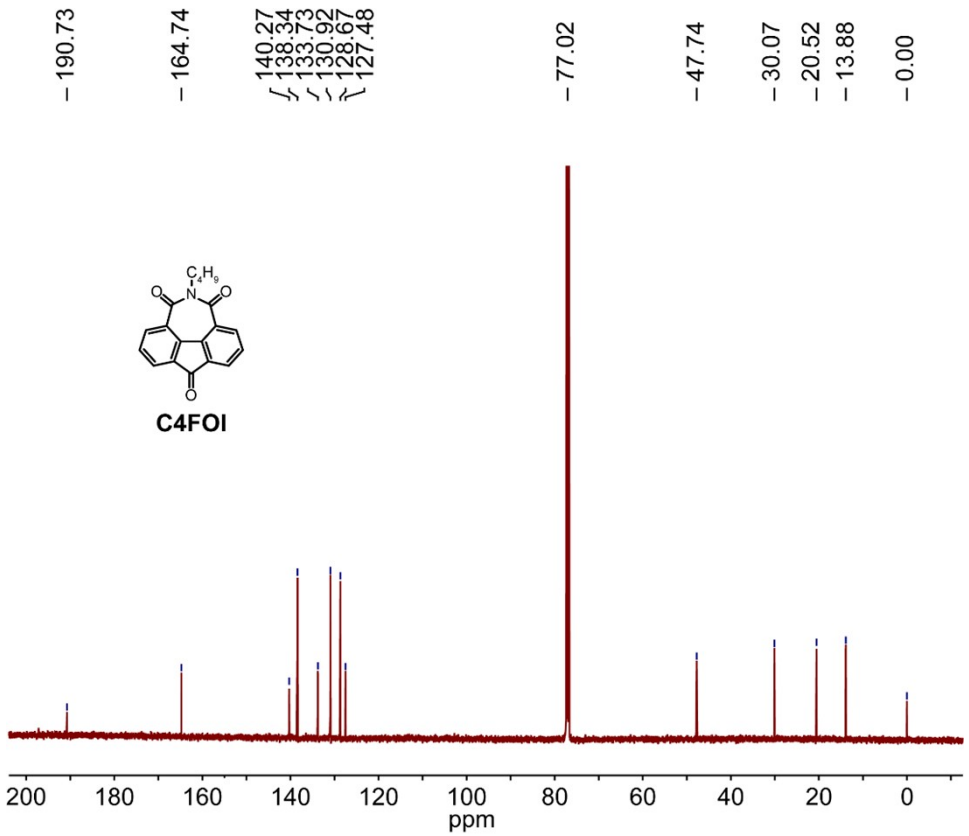

Fig. S8. ^{13}C NMR spectrum of compound **C4FOI** in $CDCl_3$.

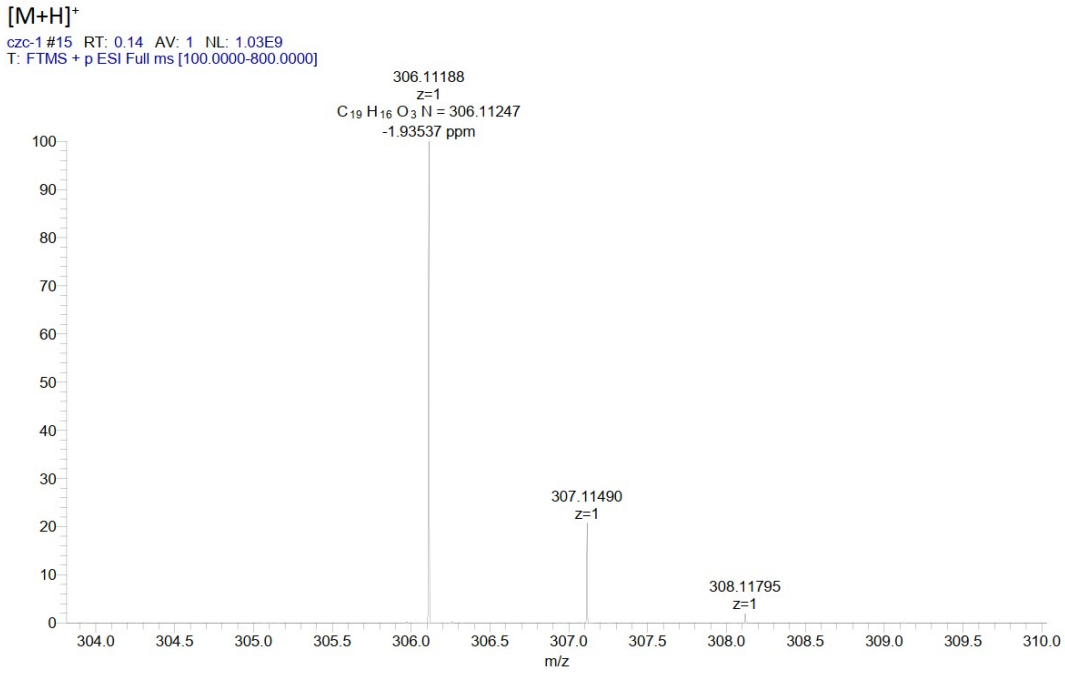

Fig. S9. High-resolution mass spectrum of compound **C4FOI** (positive mode).

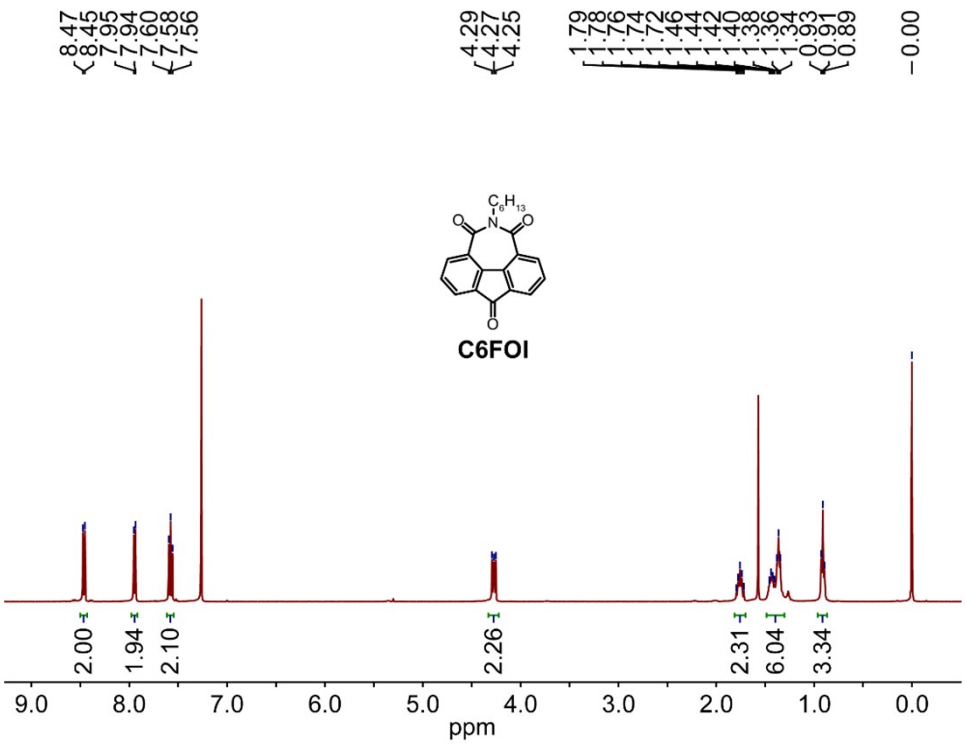

Fig. S10. ^{1}H NMR spectrum of compound **C6FOI** in $CDCl_3$.

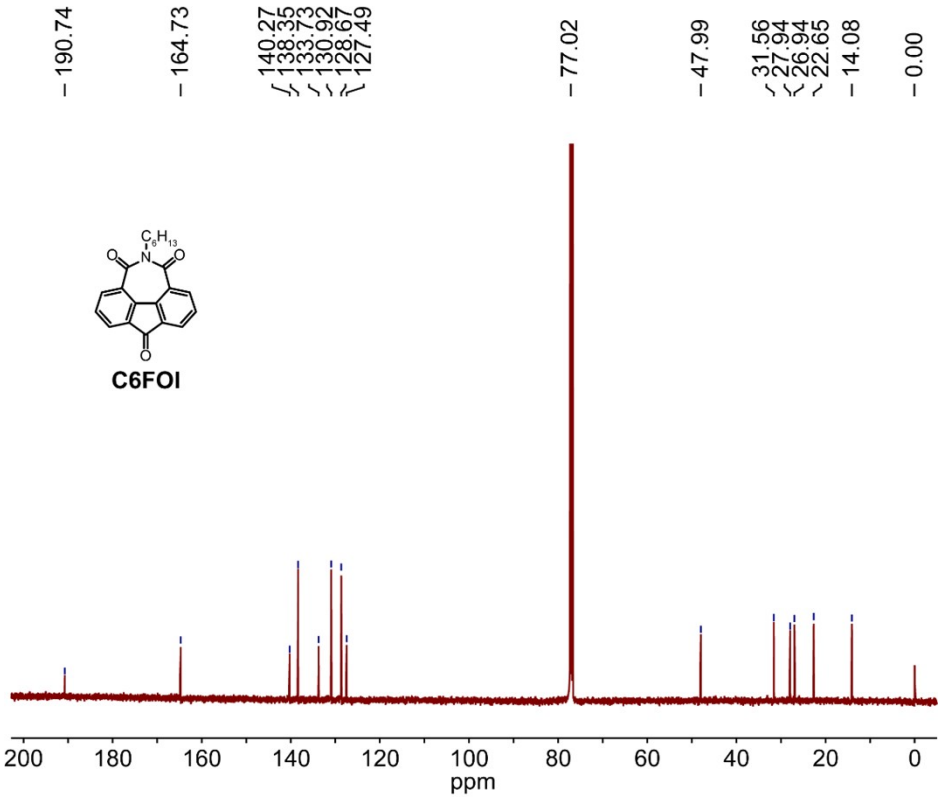

Fig. S11. ^{13}C NMR spectrum of compound **C6FOI** in $CDCl_3$.

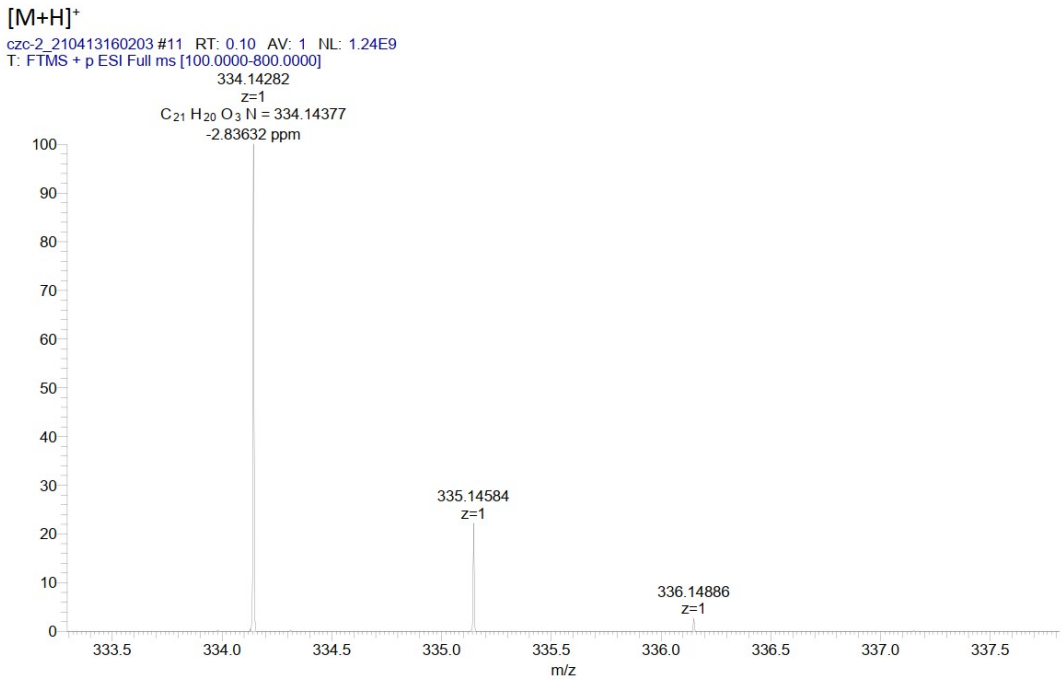

Fig. S12. High-resolution mass spectrum of compound **C6FOI** (positive mode).

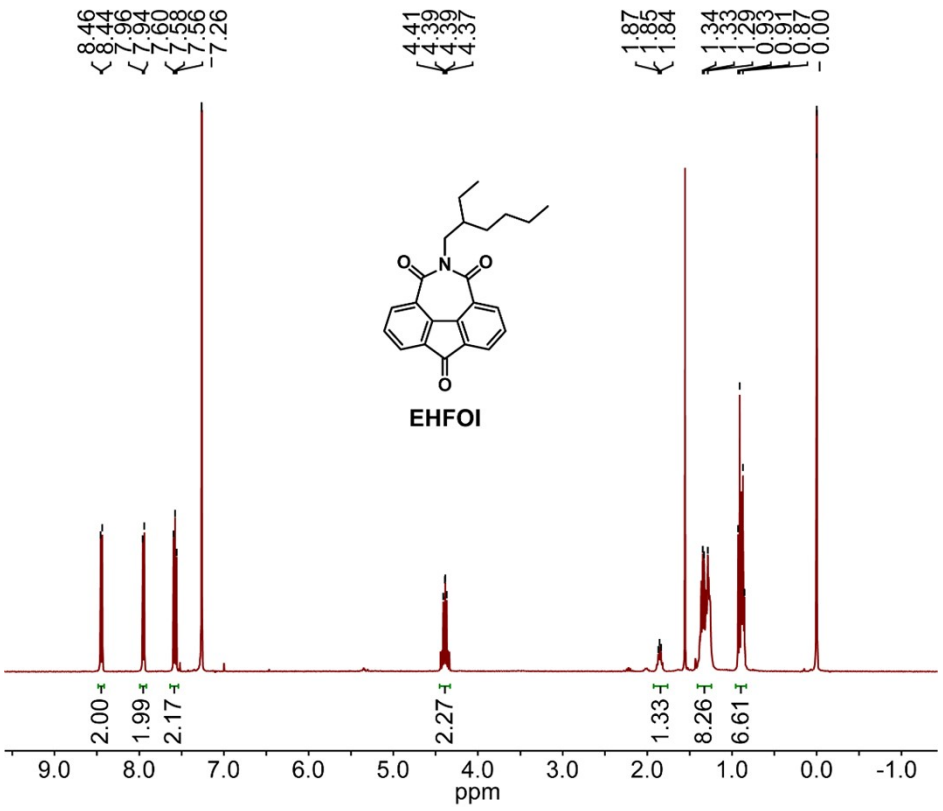

Fig. S13. ^{1}H NMR spectrum of compound **EHFOI** in $CDCl_3$.

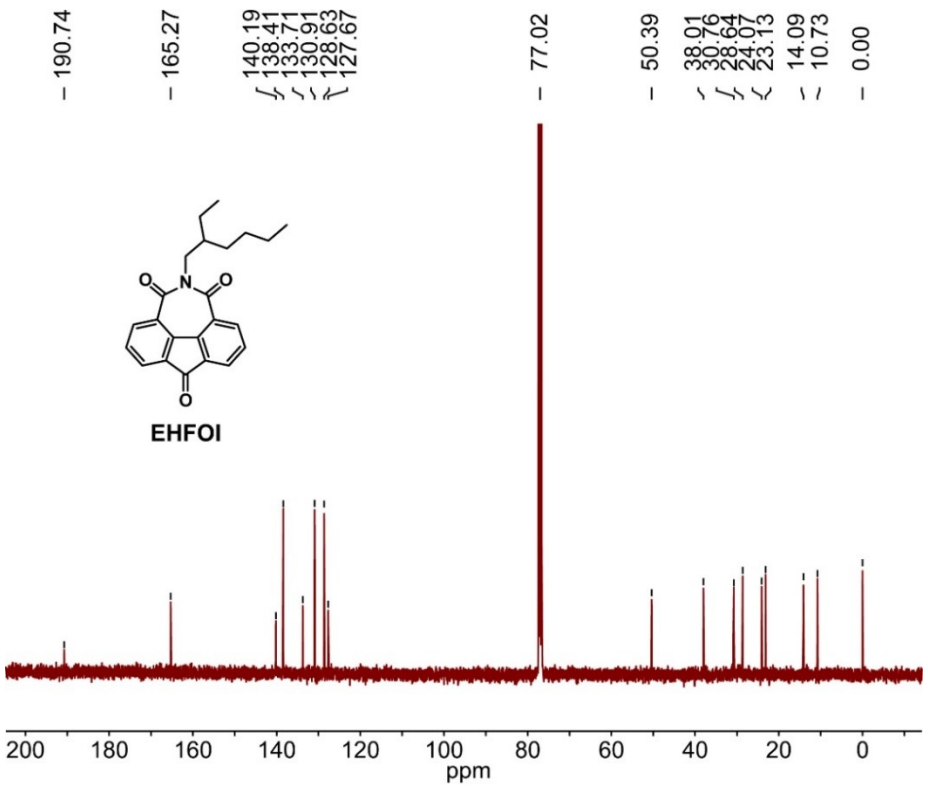

Fig. S14. ^{13}C NMR spectrum of compound **EHFOI** in $CDCl_3$.

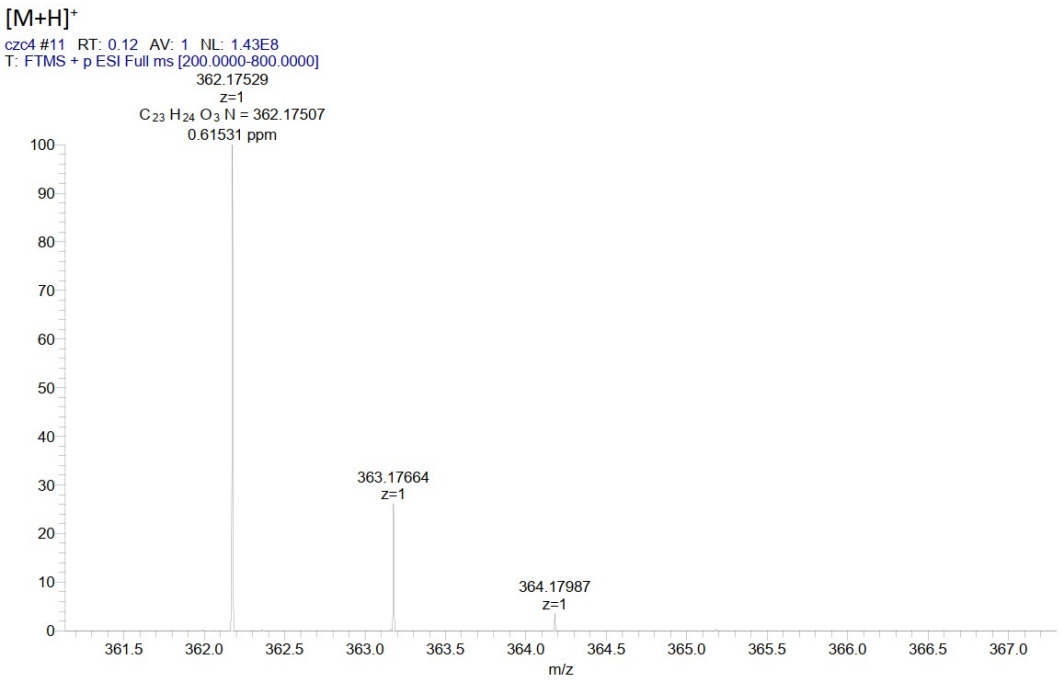

Fig. S15. High-resolution mass spectrum of compound **EHFOI** (positive mode).

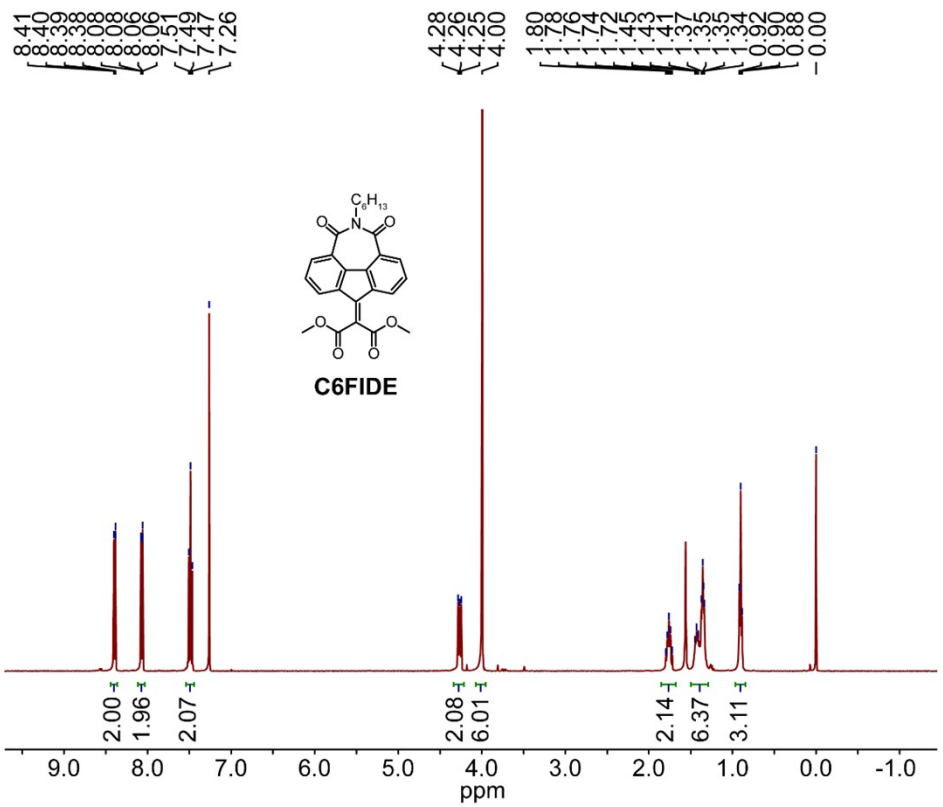

Fig. S16. ^{1}H NMR spectrum of compound **C6FIDE** in $CDCl_3$.

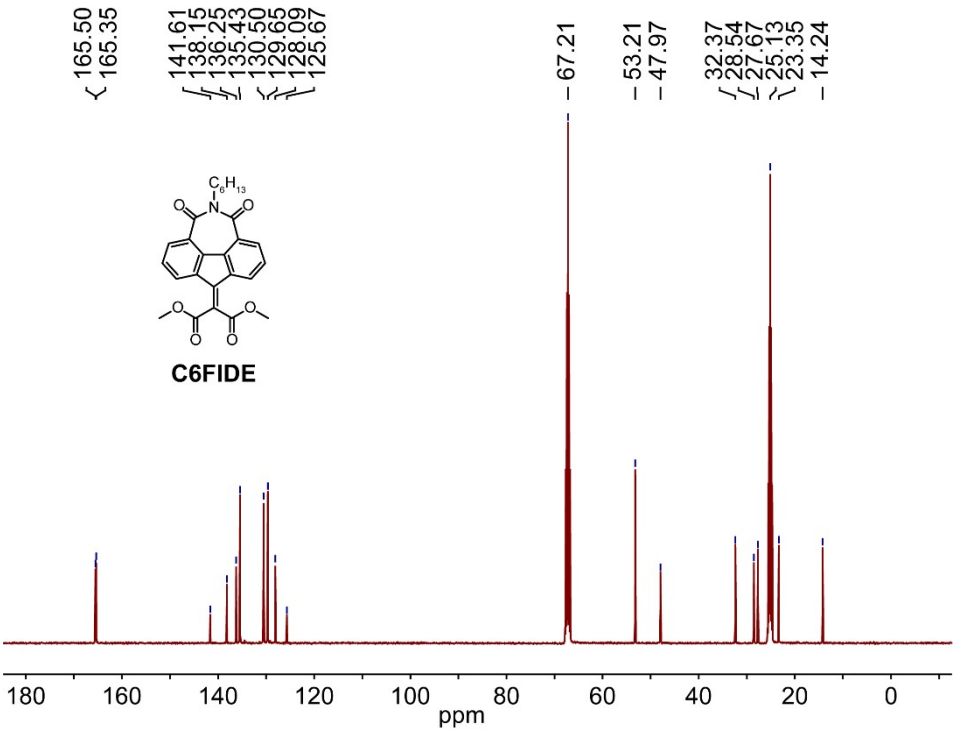

Fig. S17. ^{13}C NMR spectrum of compound **C6FIDE** in THF-d_8.

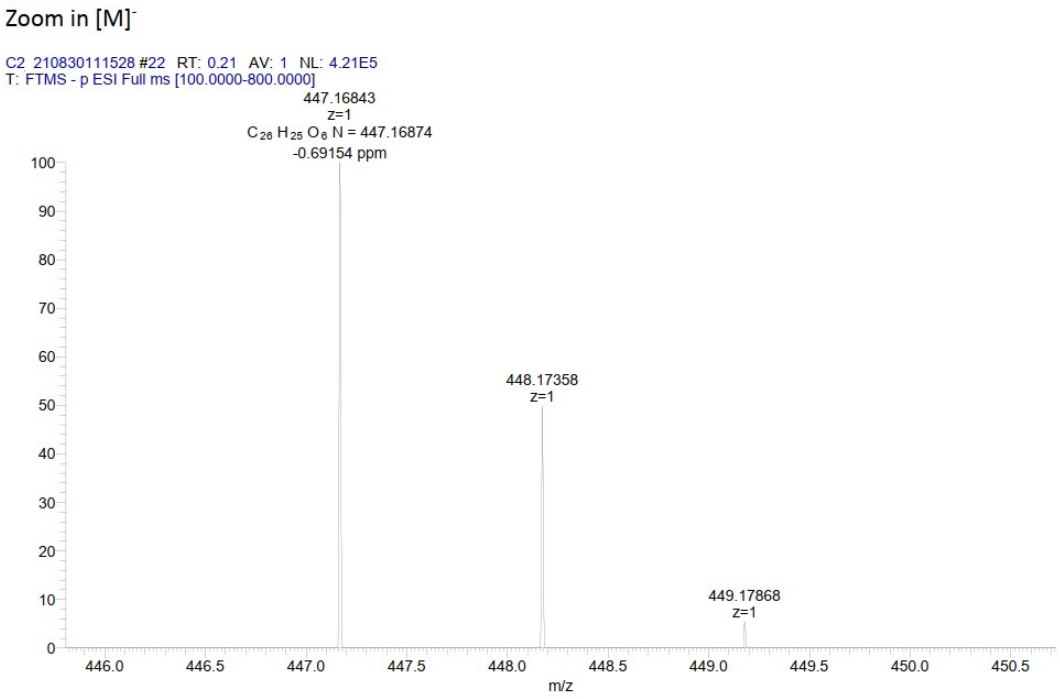

Fig. S18. High-resolution mass spectrum of compound **C6FIDE** (negative mode).

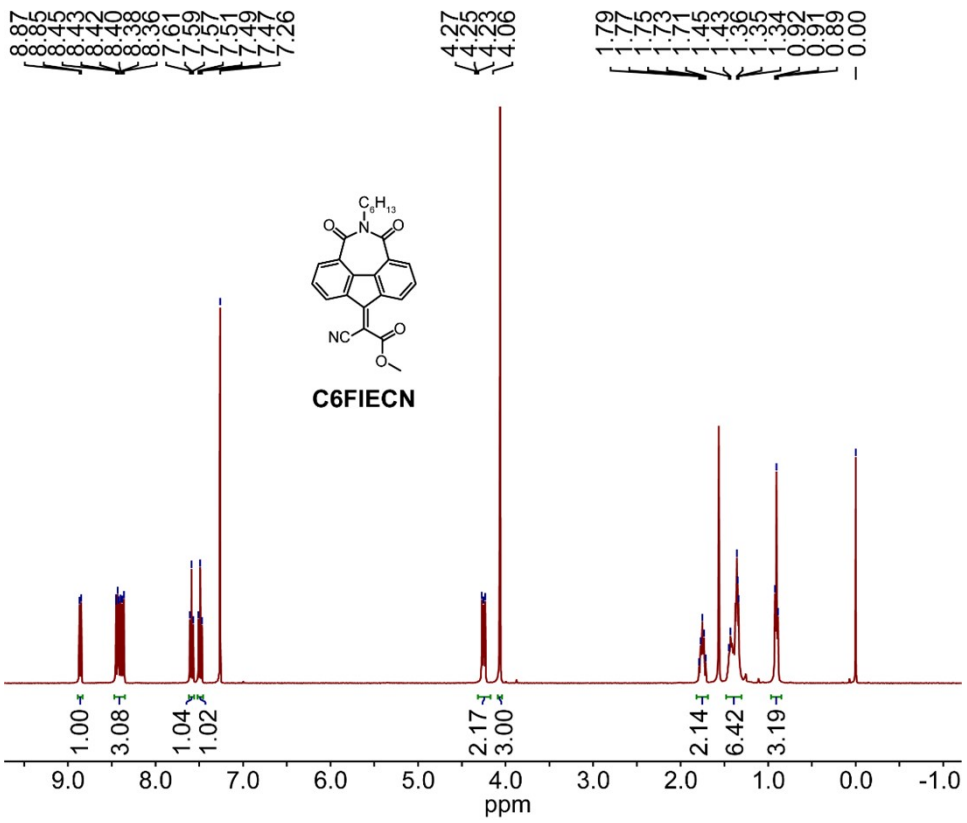

Fig. S19. ^{1}H NMR spectrum of compound **C6FICNE** in $CDCl_3$.

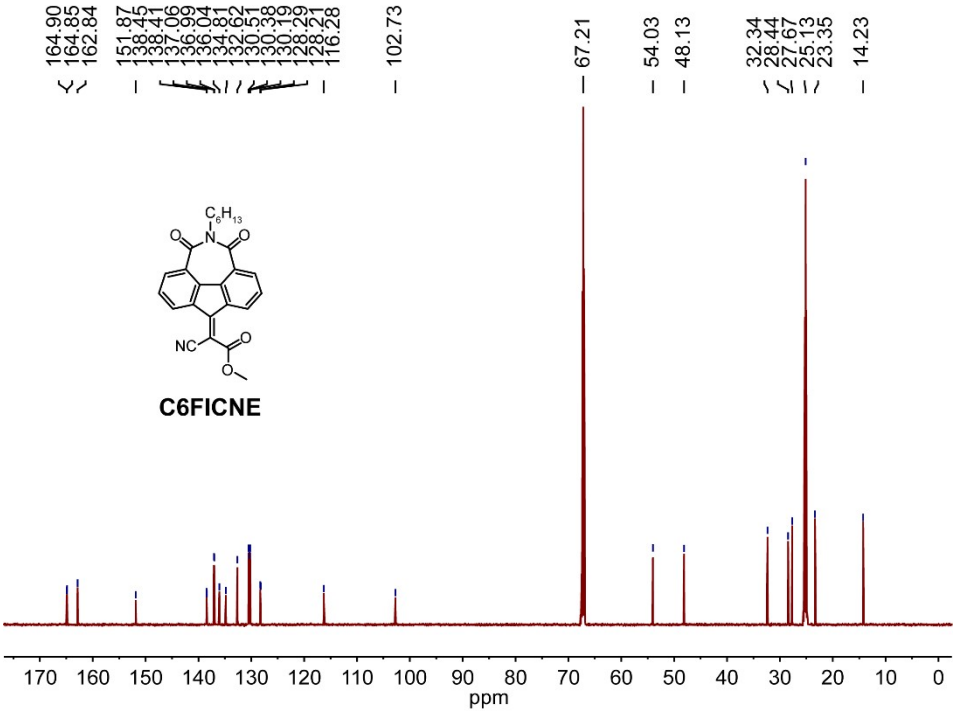

Fig. S20. ^{13}C NMR spectrum of compound **C6FICNE** in THF-d_8.

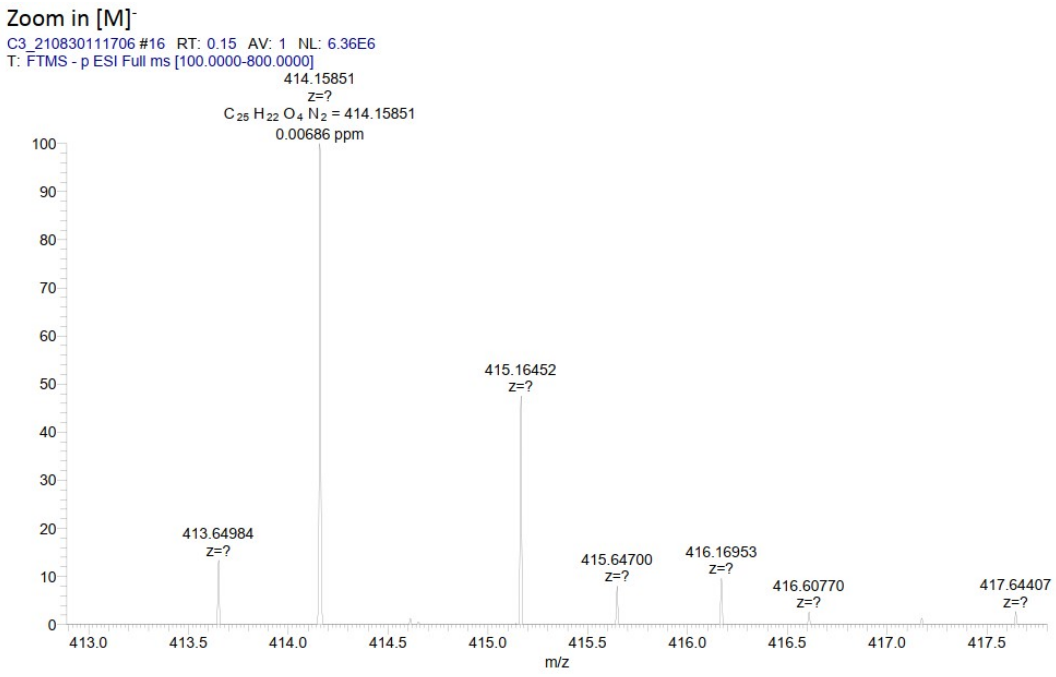

Fig. S21. High-resolution mass spectrum of compound **C6FICNE** (negative mode).

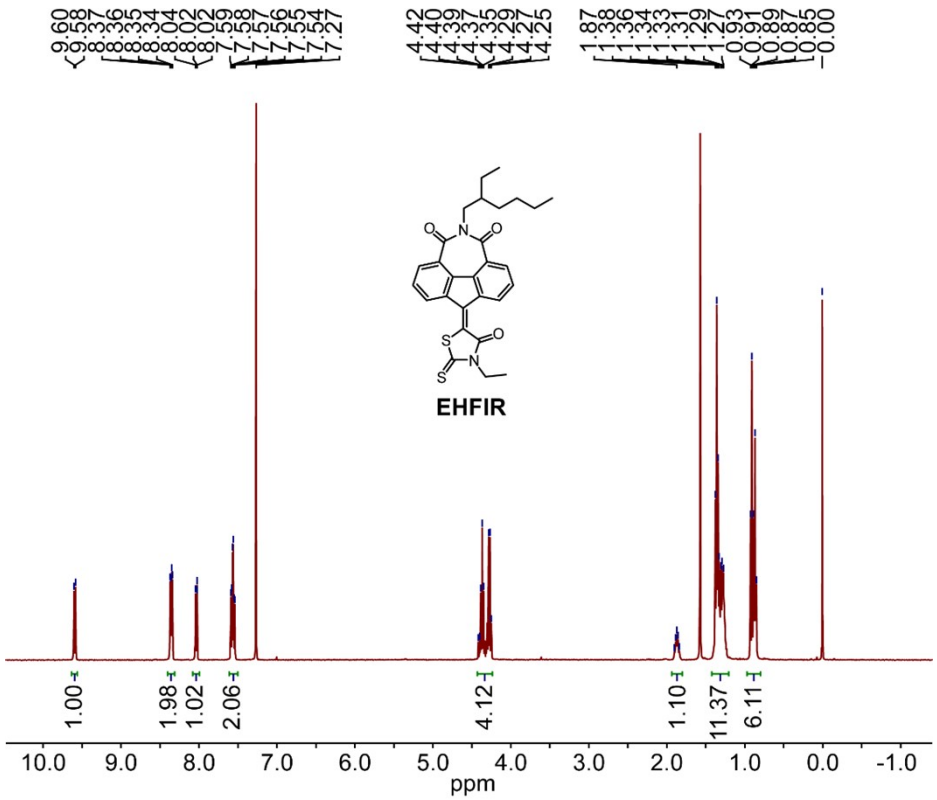

Fig. S22. ^{1}H NMR spectrum of compound **EHFIR** in $CDCl_3$.

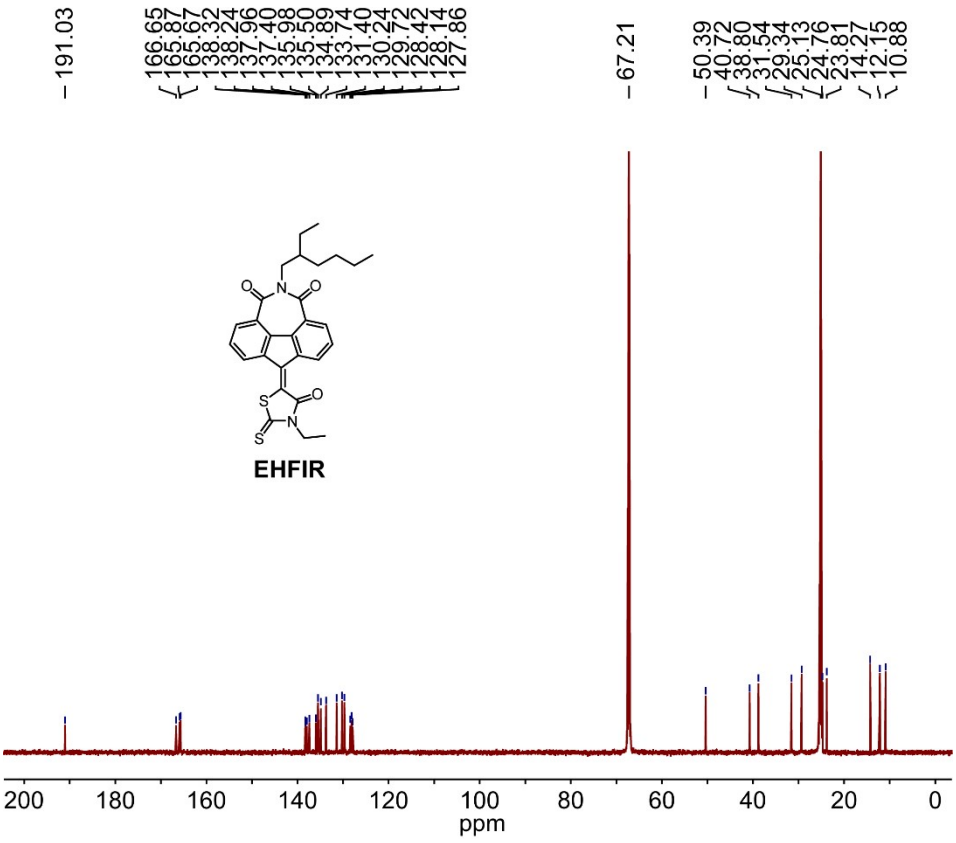

Fig. S23. ^{13}C NMR spectrum of compound **EHFIR** in THF-d_8.

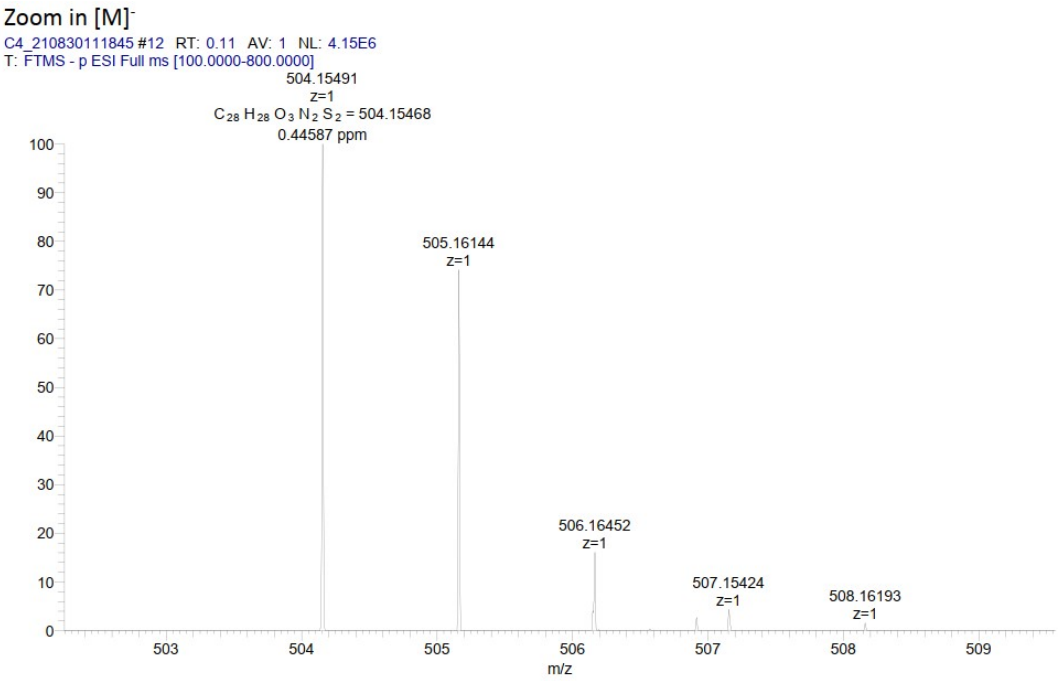

Fig. S24. High-resolution mass spectrum of compound **EHFIR** (negative mode).

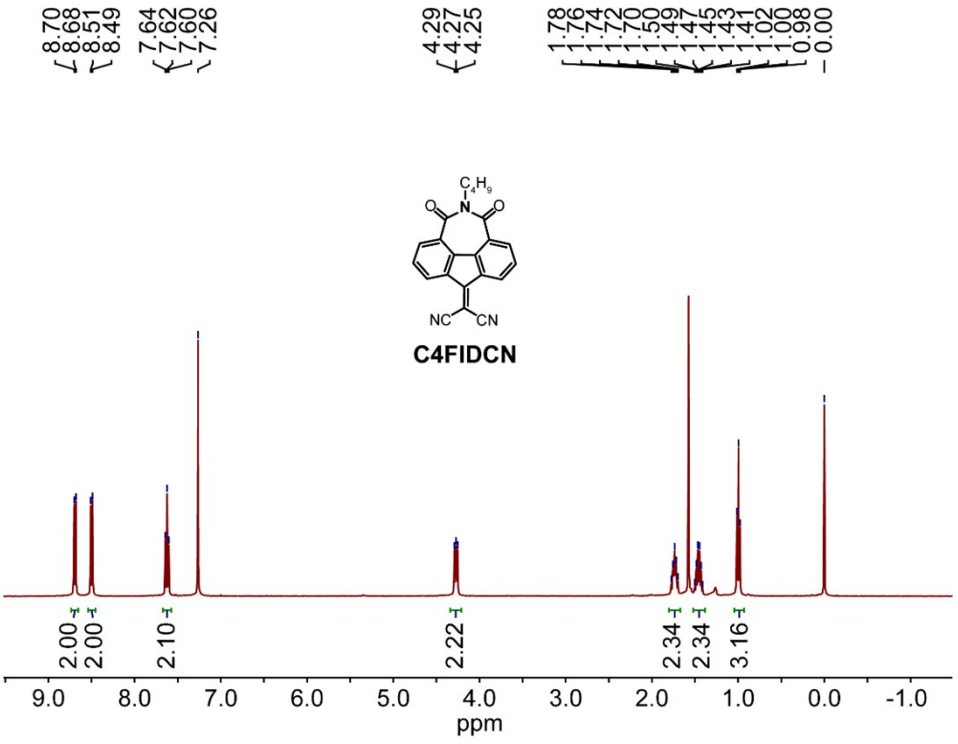

Fig. S25. ^{1}H NMR spectrum of compound **C4FIDCN** in $CDCl_3$.

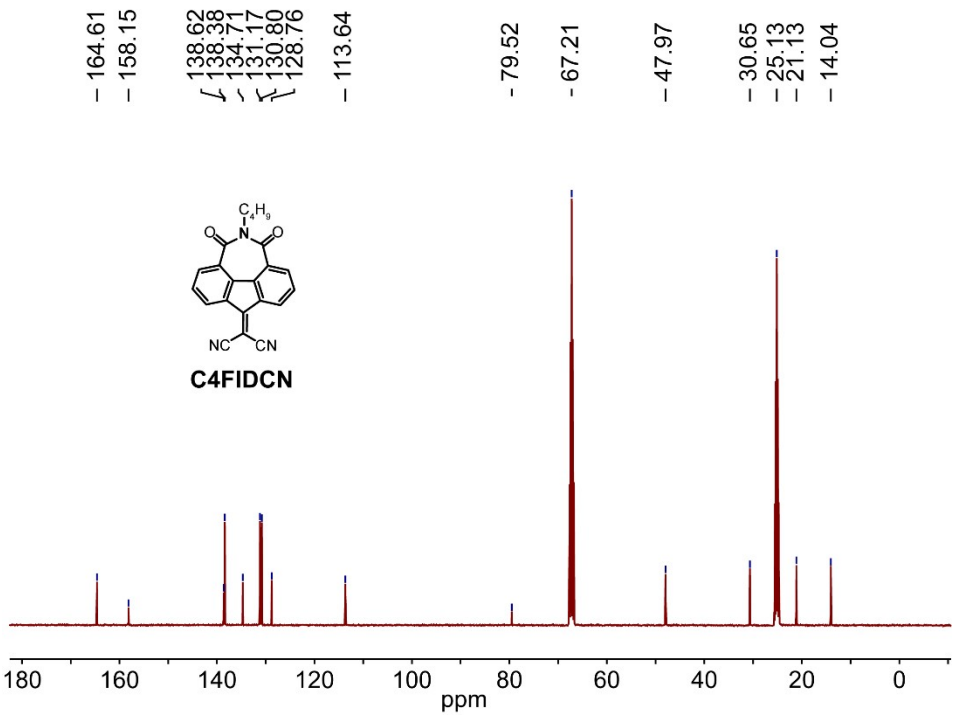

Fig. S26. ^{13}C NMR spectrum of compound **C4FIDCN** in THF-d_8.

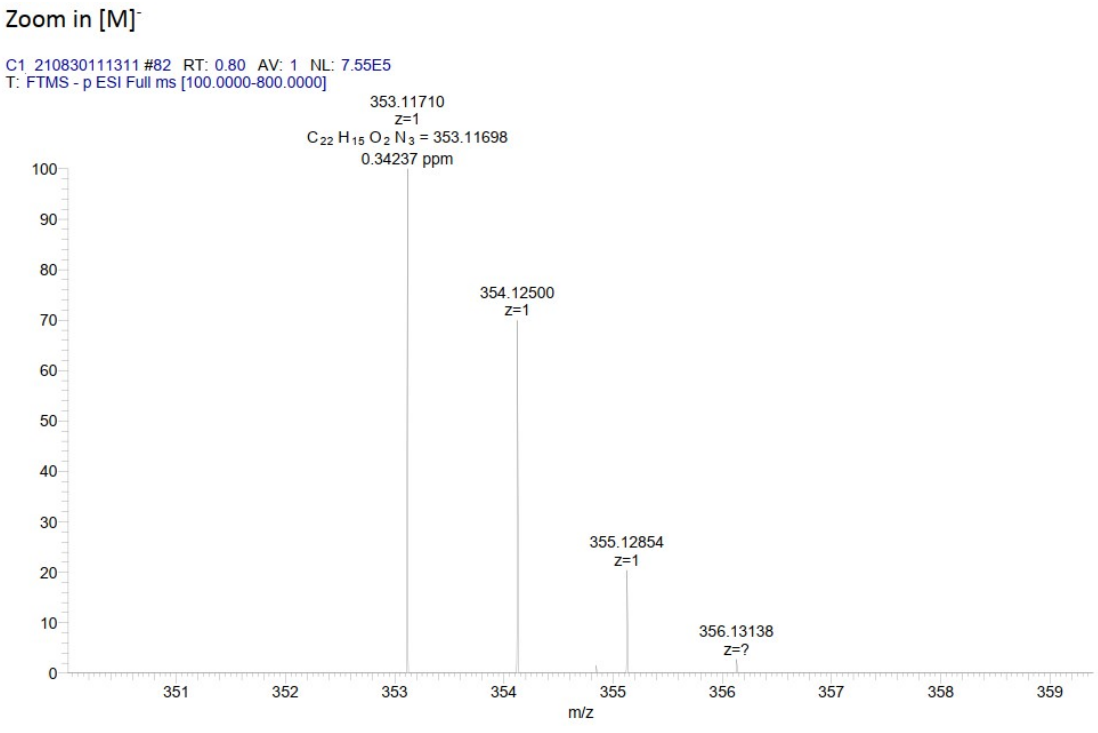

Fig. S27. High-resolution mass spectrum of compound **C4FIDCN** (negative mode).

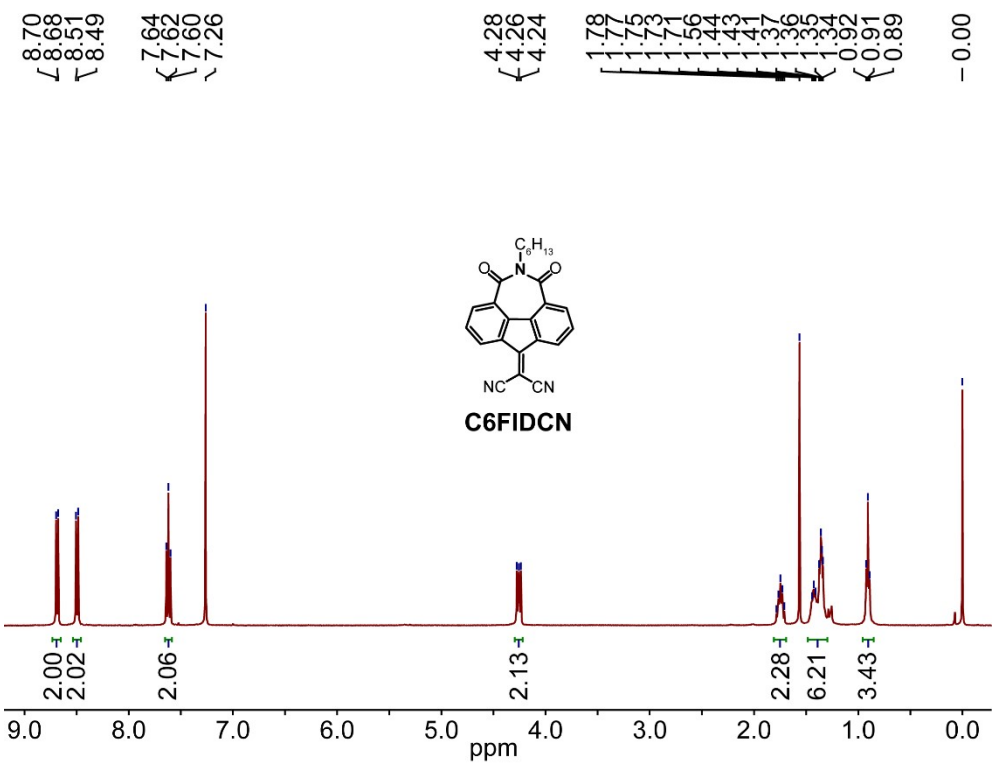

Fig. S28. ^{1}H NMR spectrum of compound **C6FIDCN** in $CDCl_3$.

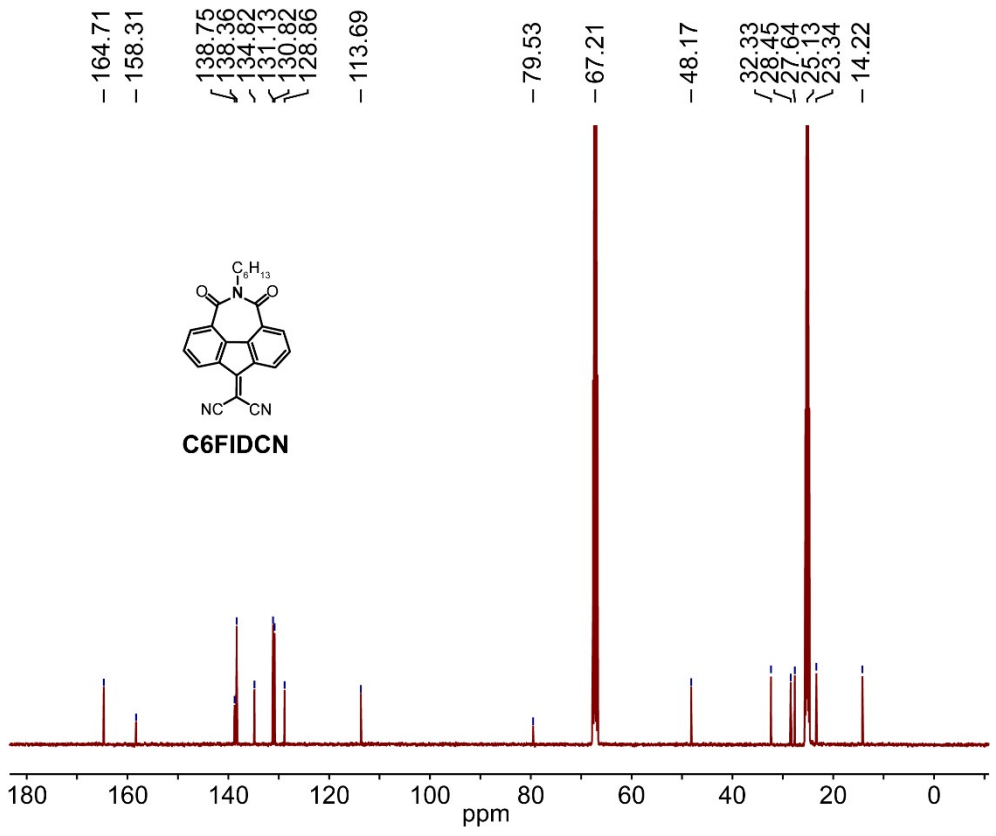

Fig. S29. ^{13}C NMR spectrum of compound **C6FIDCN** in THF-d_8.

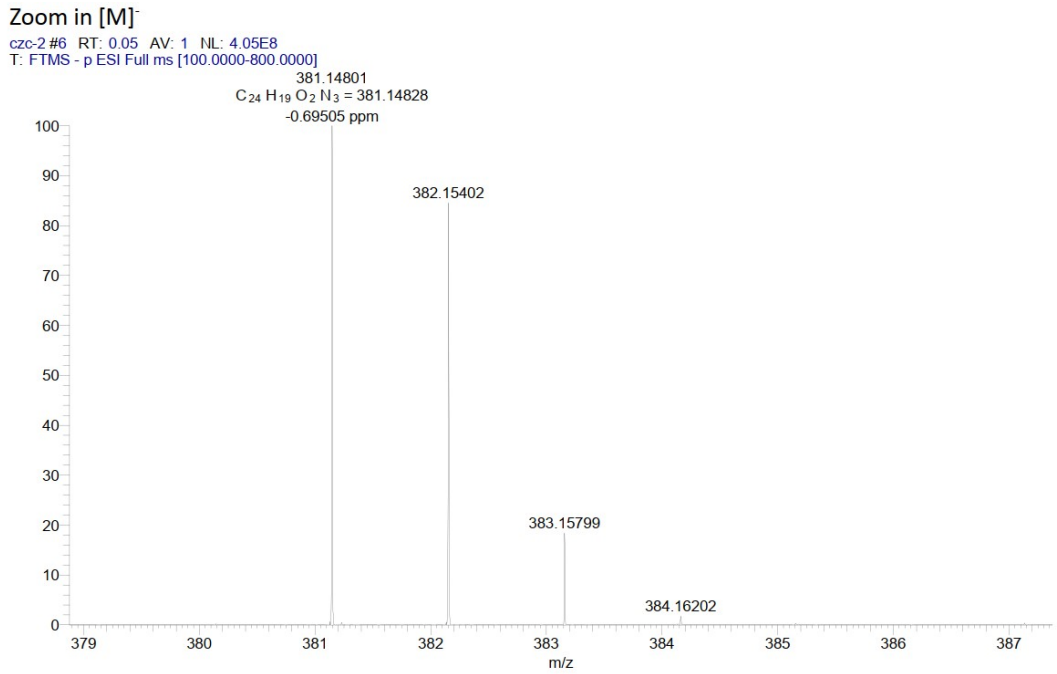

Fig. S30. High-resolution mass spectrum of compound **C6FIDCN** (negative mode).

4. Thermal properties

Thermogravimetric analysis (TGA) was performed to study the thermal properties on a Shimadzu DTG-60H thermogravimetric analyses at a heating rate of 10 °C/min under a nitrogen atmosphere. As shown in **Fig. S31**, mass losses of **C6FOI** and **C6FIDCN** go to zero, the process is more likely sublimation/evaporation, not the complete thermal decomposition. Therefore, the thermal stability of them may be even higher.

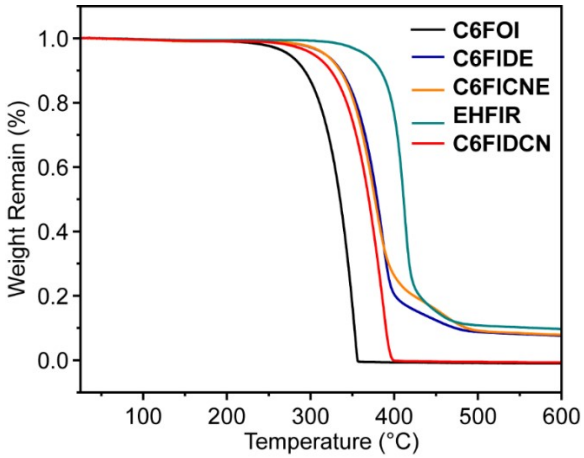

Fig. S31. TGA curves of **C6FOI**, **C6FIDE**, **C6FICNE**, **EHFR**, and **C6FIDCN**.

5. Optical properties

Photoluminescence (PL) spectra of **C6FOI**, **C6FIDE**, **C6FIECN**, **EHFIR** and **C6FIDCN** in dichloromethane (DCM) solution were record using an Edinburg LFS980 fluorescence spectrophotometer. The PL quantum yield of the molecules were measured using a Hamamatsu absolute PL quantum yield spectrometer C11347.

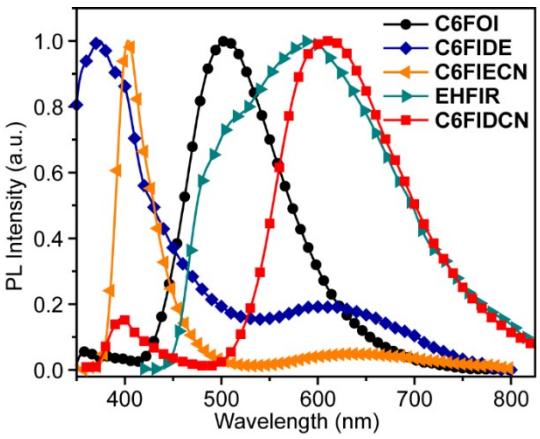

Fig. S32. PL spectra of **C6FOI**, **C6FIDE**, **C6FICNE**, **EHFIR** and **C6FIDCN** in DCM (10^{-4} M) solution (excitation wavelength: **C6FOI**/320 nm, **C6FIDE**/320 nm, **C6FICNE**/340 nm, **EHFIR**/405 nm, **C6FIDCN**/340 nm).

Table S1. Photophysical, electrochemical and thermal properties of the molecules.

Molecule	λ_{max} (nm)		PLQY (%)	T_d
	Abs.	PL		
C6FOI	324/340	505	2.1	275
C6FIDE	329	374	1.8	318
C6FICNE	345	404	1.2	317
EHFIR	432	590	0.9	366
C6FIDCN	350/367	610	0.7	303

6. Electrochemical studies

Cyclic voltammetry measurements[4] of the molecules were carried out under argon atmosphere using a CHI760E voltammetric analyzer with 0.1 M tetra-n-butylammonium hexafluorophosphate (Bu_4NPF_6) in acetonitrile as supporting electrolyte. A glassy carbon working electrode, a platinum wire counter electrode and

silver wire reference electrode were employed, and Fc/Fc^+ was used as internal reference for all measurements. The scan rate was 100 mV/s. Molecular films were drop-coated from chloroform solutions on a working electrode (2 mm in diameter). The supporting electrolyte solution was thoroughly purged with Ar before all CV measurement.

$$E_{LUMO} = - (4.80 - E_{[Fc+/Fc]} + E\text{onset red}) \text{ eV} \quad (1)$$

Where *E*onset red is the onset potential of reduction, and $E_{[Fc+/Fc]}$ is the $E_{1/2}$ of Fc^+/Fc vs AgCl/Ag, respectively.

Table S2. Photophysical, electrochemical and thermal properties of the molecules.

Molecule	(V)		(eV)					
	$E_{Fc+/Fc}$[b]	*E*onset red	HOMO[d]	LUMO[c]	*E*opt g[a]	HOMO[e]	LUMO[e]	E_g[e]
C6FOI	0.46	0.71	-7.08	3.36	3.45	-6.78	-2.72	4.06
C6FIDE	0.46	0.68	-7.07	3.66	3.41	-6.46	-2.76	3.70
C6FICNE	0.46	0.49	-7.08	3.85	3.23	-6.73	-3.25	3.48
EHFIR	0.45	0.48	-6.51	3.87	2.64	-6.46	-3.31	3.15
C6FIDCN	0.45	0.36	-7.21	3.99	3.22	-7.06	-3.63	3.43

[a] Estimated from absorption onset of the absorption spectrum using the equation: *E*opt g = $1240/\lambda_{onset}$ (eV). [b] $E_{[Fc+/Fc]}$ is the $E_{1/2}$ of Fc^+/Fc vs AgCl/Ag, here using Fc^+/Fc as internal standard, [c] $E_{LUMO} = - (4.80 - E_{[Fc+/Fc]} + E\text{onset red})$ eV, [d] Calculated based on the equation: $E_{HOMO} = E_{LUMO} - E\text{opt g}$. [e] DFT calculated.

7. Computational studies

Density functional theory (DFT) calculations were performed on Gaussian 09 program package[5] in a gas phase, using the Becke three-parameter hybrid functional combined with Becke-Lee-Yang-Parr correlation functional (B3LYP) with 6-31G(d) basis set to get theoretical prediction on the single molecular geometries, the frontier orbital energy levels, and isosurfaces of the imide-functionalized fluorenone derivatives. Vibrational frequencies analysis was performed for the optimized geometries to confirm all

stationary points are minima (zero imaginary frequencies) on the respective potential energy hypersurfaces. HOMO and LUMO energies were calculated for the optimized geometries. The all orbital surfaces were obtained using GaussView 5.0. The energy gap (E_g) was achieved from the energy difference between HOMO and LUMO of the compound. Transfer integral analysis was also carried out through theoretical calculation by Gaussian 09 software,[5] using B3LYP functional and 6-31G (d, p) basis set for modeling based on their single crystal structures.

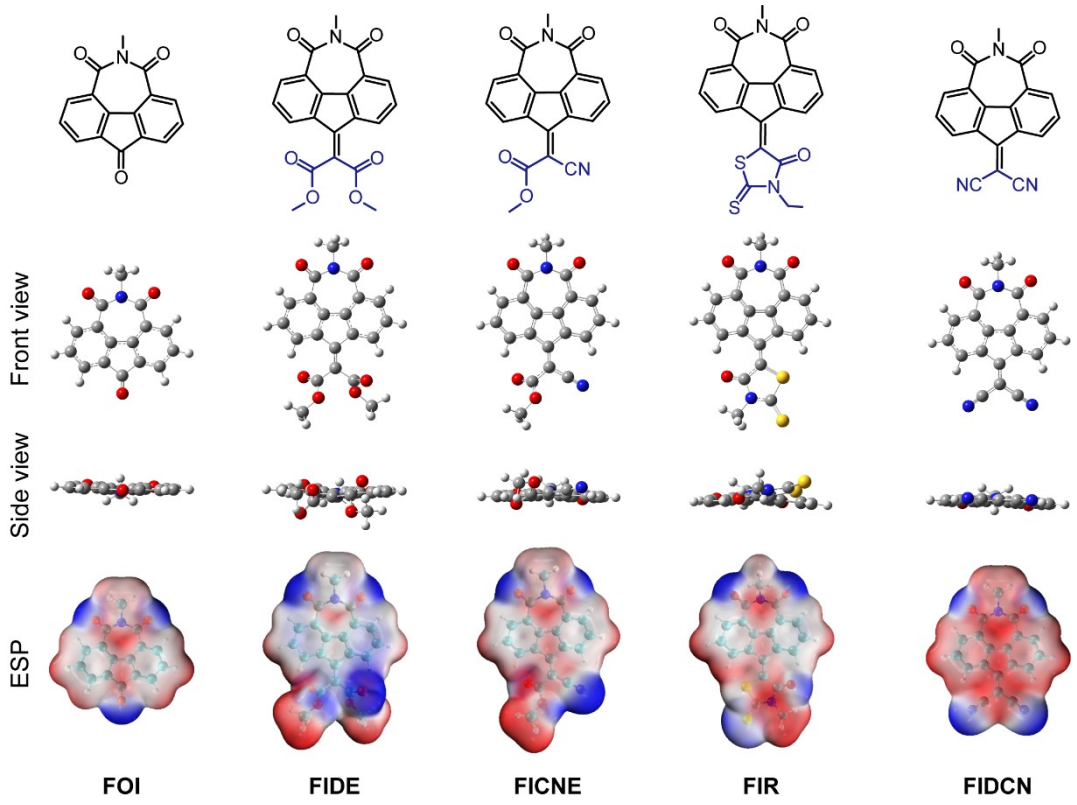

Fig. S33. Optimized molecular geometries and electrostatic potential (ESP) surface of fluorenone imide and its derivatives of fluorenone imide and its derivatives. The alkyl chains were replaced with methyl groups for calculation simplicity and the calculations were carried out at the B3LYP/6-31G (d) level.

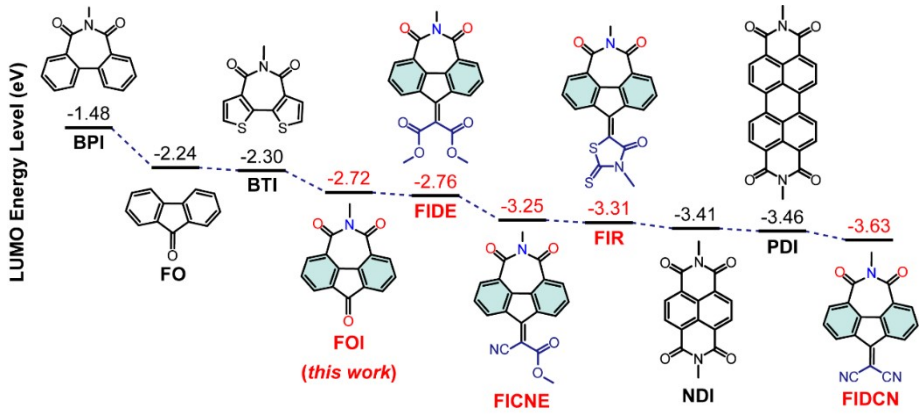

Fig. S34. The LUMO energy levels of **FOI**, **FIDE**, **FICNE**, **FIR**, and **FIDCN** together with some classic acceptor units as comparison. The LUMO levels are calculated based on density functional theory (DFT) at the B3LYP/6-31G (d) level.

Atom coordinates, total energies and HOMO/LUMO energy levels for B3LYP/6-31G(d) optimized geometries of fluorenone imide and its derivatives.

FOI

E(total)=-895.594957 Hatree
E(HOMO)=-0.24941 Hatree; E(LUMO)=-0.10031 Hatree

C	-0.58743200	-0.73210800	0.00443300
C	-1.92286100	-1.18732800	0.02793300
C	-2.83643200	0.00002100	0.05341700
C	-1.92284300	1.18735500	0.02781100
C	-0.58742000	0.73211700	0.00438800
C	-2.23313400	2.53445400	0.01218300
C	-1.17207600	3.45262100	-0.03494400
C	0.14513800	3.00883600	-0.06406100
C	0.47043500	1.63190700	-0.03884400
C	0.47040700	-1.63191800	-0.03883700
C	0.14509900	-3.00884600	-0.06393600
C	-1.17211800	-3.45261100	-0.03467400
C	-2.23316100	-2.53442700	0.01242600
C	1.92914900	1.30503200	-0.05137600
N	2.45456900	-0.00003500	0.13465500
C	1.92910900	-1.30505600	-0.05167300
O	-4.05304100	0.00003300	0.08359400
O	2.72751400	-2.22583900	-0.17096600
O	2.72759500	2.22584200	-0.17022100
C	3.92897100	-0.00003900	0.29672800
H	-3.26923000	2.85821900	0.03179200
H	-1.37615400	4.51843700	-0.05103000
H	0.96544500	3.71509900	-0.10441200
H	0.96539400	-3.71512100	-0.10433700
H	-1.37621200	-4.51842500	-0.05065200
H	-3.26925900	-2.85818300	0.03209200
H	4.21384900	0.89774300	0.83736400
H	4.21392600	-0.89800800	0.83702400
H	4.42873300	0.00013800	-0.67551000

FIDE

E(total)=-1315.416395 Hatree
E(HOMO)=-0.23776 Hatree; E(LUMO)=-0.10014 Hatree

C	-1.21781900	0.73620900	-0.04681200
C	0.12272700	1.20334400	-0.05150300
C	1.03928100	0.02802800	-0.08259700
C	0.14005000	-1.16028100	-0.15259500
C	-1.20747600	-0.71664600	-0.07698100
C	0.41074600	-2.52355400	-0.23828100
C	-0.65492500	-3.43063700	-0.23985200
C	-1.96719900	-2.99148500	-0.15036500
C	-2.27248500	-1.61823600	-0.06126400
C	-2.29758700	1.61895800	-0.08107900
C	-2.01406300	2.99830700	-0.13400500
C	-0.70647900	3.46139800	-0.14068900
C	0.37299800	2.57228500	-0.09909200
C	-3.72890200	-1.31009900	0.08540600
N	-4.25688600	-0.00843400	0.24063000
C	-3.75201500	1.27657900	-0.07208400
C	2.39962500	0.02881300	-0.02685400
O	-4.56488200	2.17412000	-0.25734400
O	-4.52086300	-2.24541900	0.11319500
C	-5.71545400	-0.00903400	0.50156400
C	3.24382600	1.24032500	0.24311600
C	3.25201000	-1.19782500	-0.20655200
O	4.32835400	1.23437000	-0.56203300
O	4.09930800	-1.32999400	0.83429800
O	3.03578100	2.09684700	1.07570500
O	3.22594900	-1.95475300	-1.15294000
C	5.27404400	2.29527800	-0.33777700
C	5.04588700	-2.40965600	0.73121900
H	1.41938000	-2.89652600	-0.33300300
H	-0.44876300	-4.49354600	-0.31531700
H	-2.79232700	-3.69233700	-0.14270100
H	-2.85069100	3.68466400	-0.17048300
H	-0.51558400	4.52915600	-0.17757900
H	1.37869300	2.96401900	-0.09132400
H	-5.94530400	-0.84732000	1.15331700
H	-5.98078700	0.93848000	0.96121900
H	-6.27980900	-0.12185200	-0.42788100
H	6.07807800	2.12492500	-1.05255700
H	4.80727200	3.26783600	-0.51002700
H	5.65180000	2.25926600	0.68666200
H	5.65340100	-2.35165800	1.63340800
H	4.52858100	-3.37037800	0.67849800
H	5.66436400	-2.28947300	-0.16121800

FICNE

E(total)=-1179.785515 Hatree
E(HOMO)=-0.24768 Hatree; E(LUMO)=-0.11954 Hatree

C	-0.88626800	0.76504400	-0.06941900
C	0.39838600	1.36774200	-0.10910300
C	1.42947800	0.29617700	-0.12728200
C	0.66909600	-0.98142200	-0.15195000
C	-0.71997900	-0.67900400	-0.07477800
C	1.08029300	-2.31190800	-0.20133900
C	0.11341500	-3.32385100	-0.17009600
C	-1.23664300	-3.02142700	-0.08980700
C	-1.68398500	-1.68413800	-0.03370400
C	-2.04878900	1.53163200	-0.08268300
C	-1.90695200	2.93437600	-0.14679900
C	-0.65539500	3.52936200	-0.18657600
C	0.51145500	2.75510900	-0.16974300
C	-3.16649200	-1.52688700	0.09937400
N	-3.82632600	-0.28834300	0.26846500
C	-3.46152100	1.04424000	-0.03466800
C	2.78568000	0.50637900	-0.04768700
O	-4.36306400	1.85903700	-0.18644800
O	-3.85697000	-2.53903300	0.11064700
C	-5.27548900	-0.44279700	0.53985400
C	3.85824500	-0.54214600	-0.14514800
O	4.93162100	-0.17991000	0.57697000
C	6.06645100	-1.06253600	0.49568200
O	3.80994700	-1.55744200	-0.80904200
C	3.32598200	1.81892400	0.13688900
N	3.80101100	2.87347700	0.27420900
H	2.12455500	-2.56816000	-0.28958500
H	0.42922000	-4.36113900	-0.21528700
H	-1.98509300	-3.80335200	-0.06447600
H	-2.81021600	3.53116700	-0.16590200
H	-0.57504100	4.61034900	-0.23520200
H	1.47203700	3.24769600	-0.21092200
H	-5.41302700	-1.31340300	1.17482000
H	-5.63108000	0.46305800	1.02193100
H	-5.83328600	-0.59234000	-0.38823800
H	6.83885800	-0.59521400	1.10429300
H	5.80974900	-2.04950300	0.88720600
H	6.39644000	-1.16352000	-0.54047300

FIR

E(total)=-1900.977857 Hatree
E(HOMO)=-0.23778 Hatree; E(LUMO)=-0.12191 Hatree

C	1.50169100	-0.71137400	-0.12959500
C	0.13901900	-1.09657100	-0.24751200
C	-0.71373400	0.11952400	-0.21558500
C	0.24190900	1.26074700	-0.19298600
C	1.56435700	0.73796700	-0.09035600
C	0.05798800	2.64210300	-0.24141600
C	1.17643900	3.48227100	-0.18386200
C	2.45746900	2.96634400	-0.07325700
C	2.67759000	1.57418100	-0.01739900
C	2.52715200	-1.65518800	-0.13139500
C	2.17201700	-3.01134200	-0.28819500
C	0.84838800	-3.39363000	-0.43918700
C	-0.17877500	-2.44238800	-0.42101100
C	4.11061300	1.17600200	0.14184200
N	4.54827400	-0.15127300	0.36426800
C	3.99294700	-1.40796500	0.03637400
C	-2.08627300	0.10181800	-0.12802500
O	4.75643300	-2.36283300	-0.04326200
O	4.96233000	2.05639900	0.14598100
C	5.98514000	-0.23135800	0.71841200
S	-3.03605400	-1.38909900	0.09424700
C	-4.57504100	-0.52802700	0.20702000
N	-4.35934200	0.81362000	0.06156700
C	-3.03482600	1.25085400	-0.14675600
O	-2.79115400	2.43136600	-0.33146000
S	-6.01481700	-1.28954500	0.44849900
C	-5.45780900	1.77818100	0.09248500
H	-0.93154700	3.05889500	-0.33456000
H	1.03312900	4.55722400	-0.22891500
H	3.32221100	3.61595200	-0.02529000
H	2.96977700	-3.74324900	-0.29474500
H	0.60216000	-4.44133800	-0.57692900
H	-1.19367000	-2.78116100	-0.57640600
H	6.23329900	0.62867800	1.33381800
H	6.15409300	-1.16387900	1.24927000
H	6.61133400	-0.21641100	-0.17739400
H	-5.97614000	1.71404300	1.05120400
H	-5.02340800	2.76630100	-0.04655900
H	-6.16827100	1.55445200	-0.70593100

FIDCN

E(total)=-1044.149394 Hatree
E(HOMO)=-0.25956 Hatree; E(LUMO)=-0.13371 Hatree

C	0.22654400	-0.72752600	-0.01916400
C	-1.12006600	-1.18103200	-0.01258900
C	-2.00627200	-0.00002400	0.00635800
C	-1.12008900	1.18099700	-0.01251600
C	0.22653100	0.72752100	-0.01914400
C	-1.40259300	2.54410200	-0.03414000
C	-0.33345000	3.44870200	-0.06957700
C	0.98004000	3.00094700	-0.08084200
C	1.28971600	1.62307600	-0.04891000
C	1.28975500	-1.62305200	-0.04891500
C	0.98011300	-3.00092800	-0.08096300
C	-0.33336700	-3.44871500	-0.06981900
C	-1.40253300	-2.54414500	-0.03433300
C	2.75075300	1.29878200	-0.03851800
N	3.27553800	0.00004500	0.16422500
C	2.75078000	-1.29873400	-0.03827900
C	-3.37988400	-0.00002400	0.03886800
O	3.54730000	-2.22171000	-0.14937600
O	3.54722200	2.22175400	-0.14999600
C	4.74683800	0.00000200	0.35294200
C	-4.16395300	-1.19677800	0.05918100
N	-4.82723000	-2.15333600	0.07610300
C	-4.16393500	1.19674000	0.05919400
N	-4.82716700	2.15333000	0.07606500
H	-2.41897700	2.91509300	-0.02843300
H	-0.53732800	4.51409000	-0.08985000
H	1.80629200	3.70024000	-0.11144800
H	1.80638500	-3.70019800	-0.11154400
H	-0.53722000	-4.51410600	-0.09020200
H	-2.41890500	-2.91516700	-0.02867400
H	5.02130300	0.89818300	0.89835100
H	5.02110300	-0.89771300	0.89921900
H	5.26361900	-0.00050300	-0.61019200

8. Single crystal

Single crystals of **C4FIDCN** and **C6FIDCN** were grown by slow evaporation of combined DCM and C_2H_5OH solutions at room temperature. X-ray crystallography was carried out on a Bruker SMART APEX-II CCD diffractometer with graphite monochromated Mo-Kα radiation at 298 or 167 K. The crystal structures were analyzed by Mercury 2020.3.0 software and the structure data were summarized in **Table S1**. The CIF files of the single crystals were also attached.

In **C4FIDCN** crystals, the molecules crystallize in the orthorhombic system with the *Iba*2 space group (Table S3) and show a molecular order dominated by edge-to-face interactions, leading to a herringbone arrangement with a short stacking distance of 3.38 and 3.45 Å (Fig. S35a). The cofacial columns are held together by H-bonds (2.62 Å) between the carbonyl oxygens and hydrogen atoms of the nearby molecule at the C3 positions. Due to the bulkiness of butyl, some adjacent molecules also show a longer distance of 6.38 Å (Fig. S35c). For **C6FIDCN**, the molecules crystallize in the triclinic system with the $P\bar{1}$ space group (Table S4), in which the molecule packs in a slipped-stack arrangement, with a mean distance of 3.41 Å between π-π faces (Fig. S35b, d). Similarly, the slipped-cofacial columns are also held together by H-bonds (2.65 Å) between carbonyl oxygens and adjacent hydrogen atoms at the 3 position. It is worth noting that the **C6FIDCN** crystals adopt a partial brick-wall packing motif which has been suggested to promote enhanced transfer integrals and facilitate the charge transport.[6] To further understand the effect of molecular packing mode on their mobility, their transfer integral (*t*) values were calculated based on the crystal packing model of **C4FIDCN** and **C6FIDC**. Indeed, **C4FIDCN** had a small negative *t* value of -7.45 meV in the π-stacking direction and a moderate negative *t* value of -19.56 meV (t_2) in the lateral direction, but **C6FIDCN** exhibited a large negative *t* value of -53.45 meV (t_3) in the π-stacking direction and a positive *t* value of 19.74 meV (t_4) in the lateral direction, indicating more balanced intermolecular overlaps (Fig. S35e, f, Table S5).[7]

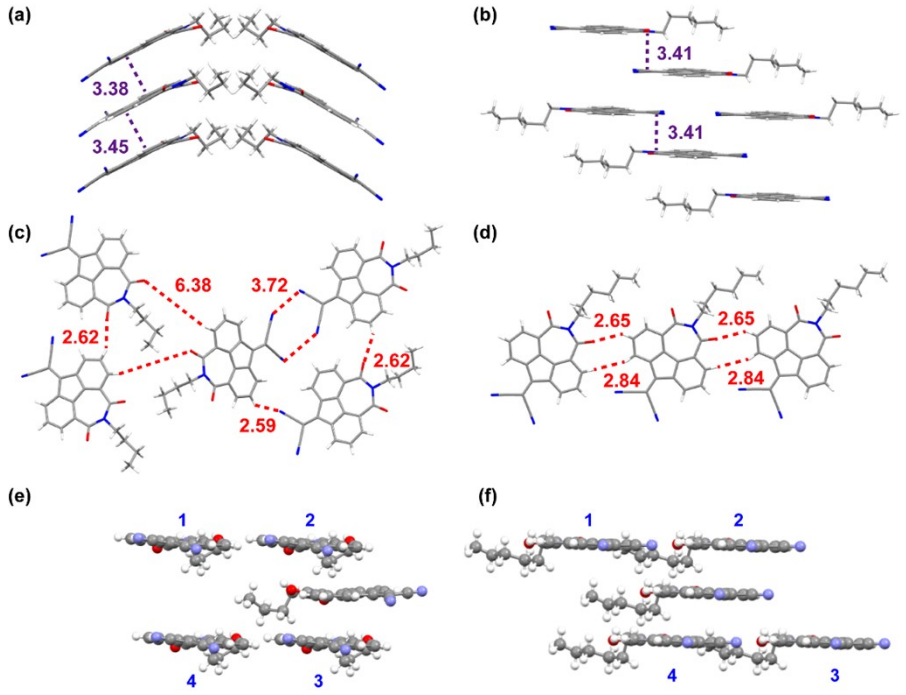

Fig. S35. Crystal packing models of **C4FIDCN** (a, c), **C6FIDCN** (distance in Å) (b, d), and short contacts and estimation of transfer integrals of **C4FIDCN** (e), **C6FIDCN** (f).

Table S3. Crystal data and structure refinement for C4FIDCN.

	C4FIDCN
Empirical formula	$C_{22}H_{15}N_3O_2$
Formula weight	353.37
Temperature/K	298(2)
Crystal system	orthorhombic
Space group	*Iba*2
a/Å	10.2240(9)
b/Å	43.467(4)
c/Å	7.7850(7) Å
α/°	90°
β/°	90°
γ/°	90°
Volume/Å^3	3459.7(5)
Z	8
ρ_{calc}g/cm^3	1.357
μ/mm^{-1}	0.089
F(000)	1472
Radiation	CuKα (λ = 1.54184)
2Θ range for data collection/°	2.812 to 28.247
Index ranges	-13 ≤ h ≤ 13, -44 ≤ k ≤ 57, -10 ≤ l ≤ 10
Reflections collected	13118
Independent reflections	4160 [R_{int} = 0.0285, R_{sigma} = 0.0097]
Data/restraints/parameters	4160/1/245
Goodness-of-fit on F^2	1.161
Final R indexes [I>=2σ (I)]	R_1 = 0.0578, wR_2 = 0.1571
Final R indexes [all data]	R_1 = 0.0805, wR_2 = 0.1783
Largest diff. peak/hole / e Å^{-3}	0.225/-0.195
CCDC NO.	2164016

Table S4. Crystal data and structure refinement for C6FIDCN.

	C6FIDCN

Empirical formula	$C_{24}H_{19}N_3O_2$
Formula weight	381.42
Temperature/K	169.98(10)
Crystal system	triclinic
Space group	$P\bar{1}$
a/Å	4.96443(14)
b/Å	9.1287(2)
c/Å	21.2708(6)
α/°	80.708(2)
β/°	88.385(2)
γ/°	88.576(2)
Volume/Å^3	950.74(4)
Z	2
ρ_{calc}g/cm^3	1.332
μ/mm^{-1}	0.694
F(000)	400.0
Crystal size/mm^3	0.15 × 0.1 × 0.08
Radiation	CuKα (λ = 1.54184)
2Θ range for data collection/°	4.21 to 135.972
Index ranges	$-4 \le h \le 5$, $-10 \le k \le 10$, $-25 \le l \le 24$
Reflections collected	10550
Independent reflections	3433 [R_{int} = 0.0360, R_{sigma} = 0.0397]
Data/restraints/parameters	3433/0/264
Goodness-of-fit on F^2	1.050
Final R indexes [I>=2σ (I)]	R_1 = 0.0544, wR_2 = 0.1457
Final R indexes [all data]	R_1 = 0.0631, wR_2 = 0.1521
Largest diff. peak/hole / e Å^{-3}	0.47/-0.20
CCDC NO.	2165586

Table S5. Short contacts and estimation of transfer integrals of **C4FIDCN** and **C6FIDCN**.

C4FIDCN	T (meV)	Ang (Å)	**C6FIDCN**	T (meV)	Ang (Å)
1	-19.56 (t_2)	3.89	**1**	19.74 (t_4)	9.12
2	-7.45 (t_1)	10.81	**2**	-53.45 (t_3)	5.01
3	-7.45 (t_1)	10.81	**3**	19.74 (t_4)	9.12
4	-19.56 (t_2)	3.89	**4**	-53.45 (t_3)	5.01

9. Device fabrication and characterization

The OFFT devices based on **C4FIDCN** and **C6FIDCN** were prepared as follows: heavily doped n-type silicon wafers with 300 nm thick SiO_2 layer (C=11 nF cm^{-2}) were successively cleaned by deionized water, piranha solution (hydrogen peroxide : concentrated sulfuric acid (1:2; v/v)), pure water and isopropanol and finally dried by nitrogen flow. Then the SiO_2 (300 nm)/Si substrate was modified with a self-assembled monolayer of orthotrichlorosilane (OTS) to optimize the surface contact quality to enhance the devices performance. Dropping the chloroform solutions of **C4FIDCN** and **C6FIDCN** (0.5 mg mL^{-1}) onto the 1 cm*1 cm above-prepared substrates which were placed in a closed jar. Then ribbon-like microcrystals were grown slowly at room temperature in the atmosphere as the solvent evaporated. And then bottom-gate/top-contact devices with Ag (80 nm) as the source and drain electrodes were fabricated by an "organic ribbon mask" technique [8-11]. More than ten devices of each material (**C4FIDCN**, **C6FIDCN**) were fabricated. Then all electrical measurements of OFETs were performed on PDA FS-Pro 380 test system with micromanipulator probe station in glove box. All the field-effect mobilities were calculated in the saturation regime of the curves based on the equation: $I_{DS} = WC_i\mu\ (V_G\text{-}V_{th})^2/2L$. In the OFET devices along the OFET channel length, the crystal of **C6FIDCN** grown along the most tightly packed direction, and the charge transport is also along this direction, which is well matching to the transfer integral analysis. **C6FIDCN** shows a 1D slipped stack motif, in which the molecule packs in a slipped-stack arrangement, with a mean distance of 3.41 Å between π-π faces. Such a packing motif is beneficial for the efficient in-plane charge transport in OFETs,[12, 13] enabling the superior device performance of **C6FIDCN**. The

mobilities of all devices based on **C6FIDCN** are on the order of 10^{-3} cm^2 V^{-1} s^{-1}, while the performances of **C4FIDCN** are poorer with no obvious field-effect transistor performance.

Table S6. OFET performance parameters of **C6FIDCN**.

Molecule	$\mu_{e,\,sat}$ (cm^2 $V^{-1}s^{-1}$) [a]	V_{th} (V) [b]	I_{on}/I_{off}
C6FIDCN	0.0071(0.0036)	6	10^4

[a] Maximum mobility with average value from at least five devices is shown in parentheses. [b] Average threshold values is shown.

10. Optical microscopy and X-ray diffraction

The optical images of all single crystals were captured by Olympus BX53, The X-ray diffraction patterns were tested by Empyrean.

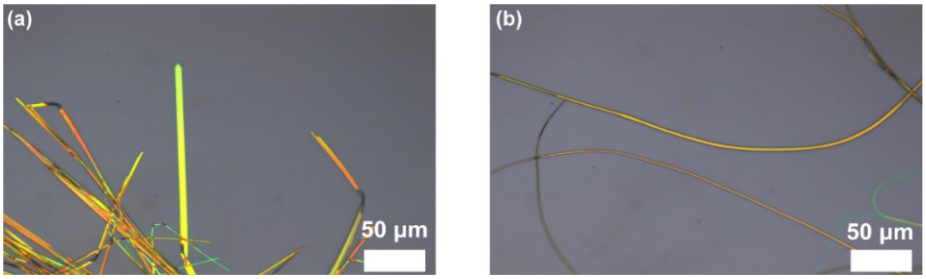

Fig. S36. Optical images of **C4FIDCN** (a) and **C6FIDCN** (b) nanowire crystals on the OTS-modified SiO_2/Si substrate.

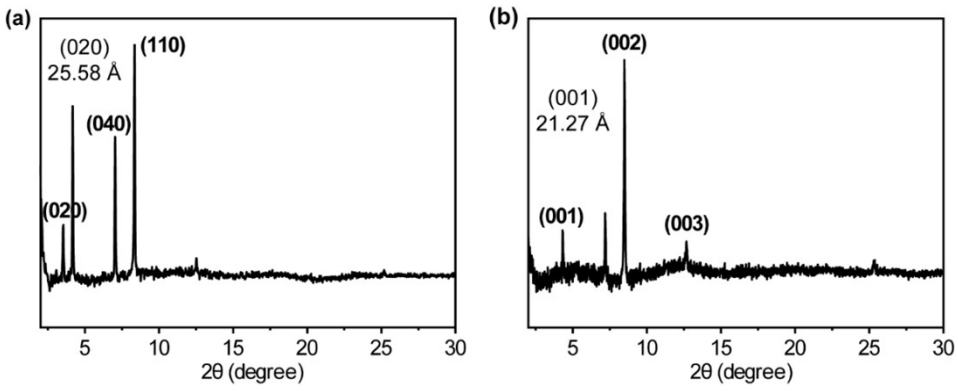

Fig. S37. X-ray diffraction pattern of **C4FIDCN** (a) and **C6FIDCN** (b) nanowire

crystals.

11. References

1. R. Deng, J. Xi, Q. Li, Z. Gu, *Chem*, 2019, **5**, 1834-1846.

2. C. Chen, P. Li, Z. Hu, H. Wang, H. Zhu, X. Hu, Y. Wang, H. Lv, X. Zhang. *Org Chem Front.*, 2014, **1**, 947-951.

3. T. P. C. Mulholland, G. Ward, *J Chem Soc*, 1956, 2415-2417.

4. C. M. Cardona, W. Li, A. E. Kaifer, D. Stockdale, G. C. Bazan, *Adv. Mater.* 2011, **23**, 2367-2371.

5. M. J. Frisch, G. W. Trucks, H. B. Schlegel, Gaussian 09, Revision A.01, Gaussian, Wallingford, Con, USA, 2009.

6. Y. Li, Z. Yao, J. Xie, H. Han, G. Yang, X. Bai, J. Pei and D. Zhao, *J. Mater. Chem. C*, 2021, **9**, 7599-7606.

7. M. Chu, J. X. Fan, S. Yang, D. Liu, C. F. Ng, H. Dong, A. M. Ren and Q. Miao, *Adv. Mater.*, 2018, **30**, 1803467.

8. H. Dong, S. Jiang, L. Jiang, Y. Liu, H. Li, W. Hu, E. Wang, S. Yan, Z. Wei, W. Xu, X. Gong, *J Am Chem Soc.*, 2009, **131**, 17315-17320.

9. R. Li, L. Jiang, Q. Meng, J. Gao, H. Li, Q. Tang, M. He, W. Hu, Y. Liu, D. Zhu, *Adv. Mater.,* 2009, **21**, 4492-4495.

10. L. Jiang, J, Gao, E. Wang, H. Li, Z. Wang, W. Hu, L. Jiang, *Adv. Mater.,* 2008, **20**, 2735-2740.

11. Y. Min, C. Dou, D. Liu, H. Dong, J. Liu, *J. Am. Chem. Soc.* 2019, 141, 42, 17015-17021.

12. M. R. Niazi, E. Hamzehpoor, P. Ghamari, I. F. Perepichka and D. F. Perepichka, *Chem. Commun.*, 2020, **56**, 6432-6435.

13. J. E. Anthony, *Chem. Rev.* 2006, **106**, 5028-5048.